

UNITED STATES DEPARTMENT OF THE INTERIOR
GEOLOGICAL SURVEY

Description of a Fresh Water Lens
at Laura Island, Majuro Atoll, Republic of the Marshall Islands,
using Electromagnetic Profiling

by

1
Jim Kauahikaua

Open-File Report 87-582

This report is preliminary and has not been reviewed for conformity with U.S. Geological Survey editorial standards and stratigraphic nomenclature. The use of trade names is solely for descriptive purposes and does not imply endorsement by the Geological Survey.

1987

1
Hawaii National Park, HI 96718

Abstract

In April 1984, electromagnetic profiling/sounding was used to estimate the configuration of a fresh water lens beneath Laura, Majuro Atoll, Republic of the Marshall Islands. Five months later, a network of monitor wells were installed in the same area to observe the lens over time. In October 1986, three of the 1984 profiles were remeasured to 1) observe changes since 1984, and 2) have one set of geoelectric data that was obtained at the same time as one set of monitor well measurements. The results show that 1) there is a large lens-shaped volume beneath Laura which extends below sea level where low resistivities indicative of seawater-saturation are absent, and 2) this volume increased in vertical thickness by up to 3 m in the 30 months between EM measurements.

Introduction

Laura is a roughly triangle-shaped island at the western end of Majuro Atoll in the Republic of the Marshall Islands (Figure 1). It is a low coralline island and is known to have a thick fresh-water lens (Huxel, 1973). The goal of this study is to estimate the size and configuration of the present fresh water lens beneath Laura. This Open-File Report describes the experimental use of electromagnetic (EM) soundings for this purpose.

Fresh-water Lens

On the larger coralline atoll islets, such as Laura, fresh ground water is stored as a lens-shaped body (Ghyben-Herzberg lens) floating on denser sea water beneath the island's surface. Both the water table and the zone between the fresh and sea water are slightly curved, meeting at the coast. The water table is convex up and the fresh/sea water interface is convex down. The curvature is greater for the lower boundary; for every meter that the water table is buoyed above sea level, the top of the sea water is depressed 40 meters below sea level. Other hydrologic properties of such lenses are described in Visher and Mink (1964) and Davis and DeWiest (1966, p. 238-240).

The transition from fresh water to sea water is gradual. The transition zone is thicker for lenses which are disturbed by strong tidal effects or pumping of wells, and is thinner for less-disturbed lenses. For Laura, transition zone thicknesses (vertical distance between the 300 to 18,000 mg/l isochlor) are typically 5 to 7 m (S. Hamlin, written communication, 1985).

Geophysical determination of lens configuration

Electrical geophysical techniques are the only ones that are sensitive to salinity changes. The resistivity of the coralline material saturated by sea water (chloride content of about 18,000 mg/l) is expected to be about 1 ohm-m (Kauahikaua, 1986). Because water resistivity is approximately inversely

proportional to salinity and bulk material resistivity is proportional to the saturating fluid resistivity (Keller and Frischknecht, 1966), we can estimate that the resistivity of the fresh water (chloride content of less than 500 mg/l)-saturated material should be greater than $(18,000/500) * 1$ ohm-m or 36 ohm-m (the asterisk means multiplication). This large a resistivity contrast (36 to 1) should be very easy to detect using electrical geophysical methods. In the application of Schlumberger and EM sounding to study the water resources of a coralline island in the Truk lagoon (Kauahikaua, 1986), the EM method yielded the most consistent results. In the Truk atoll island study, the EM data were used to determine the depth to the top of a conductive surface interpreted to be within the transition zone.

The chosen application of the EM method, generically called the slingram technique, requires two loops carried by personnel along accessible roads and trails. Equipment sets are available commercially for this purpose; the set used on Laura was an Apex Parametrics Max/Min II. Of the several modes in which the equipment might be used, the horizontal, coplanar loop mode was chosen for speed and simplicity. The two loops were separated by a constant distance of 61 m (200 ft). Data were gathered by traversing a profile with the two loops on line. Stations were 61 m apart along the profiles. At each station, the in-phase (IP) and out-of-phase (OP) or quadrature components of the mutual impedance between the loops were measured for each of five frequencies (222, 444, 888, 1777, and 3555 Hz).

EM profiling using frequencies between 222 and 3555 Hz and a loop separation of 61 m can not resolve resistivities much over 200 ohm-m. The material saturated with very fresh water (chloride content less than 90 mg/l) and non-saturated material will appear 'invisible' to this type of geophysical equipment. The air between the loops and ground, the highly-resistive ground above the water table, and the fresh water-saturated island material can be combined conceptually into a single, non-conductive geoelectric layer, greatly simplifying analysis.

The choice of separation between the two loops also sets the range of depths at which the equipment will have the highest resolution. Mundry (1967) shows that the range of depths that can usefully be explored is between 1/16 and 1/2 the loop separation. A choice of 61 m for loop separation means a depth of exploration between 4 and 30 m, a good depth interval for this study.

The theoretical response of electromagnetic systems (horizontal, coplanar loops, in particular) is not linearly related to the sensed resistivities (Keller and Frischknecht, 1966; Wait, 1982). Examples of typical responses are shown in Figure 3 where the in-phase data are plotted against the quadrature data. The in-phase and quadrature components would be one and zero, respectively, in the absence of electrically-conductive material.

In April 1984, slingram data were obtained at 196 stations on Laura island (profile lines shown in Figure 4). For the October 1986 survey, Schlumberger soundings and repeat slingram measurements were obtained at each of the monitor well locations for comparison with the hydrologic data and the 1984 EM data. The Schlumberger soundings can be used to resolve the finer details of the unsaturated and the fresh water-saturated sediments (Kauahikaua, 1986).

Interpretation

Interpretation of the electromagnetic and Schlumberger data are performed using a nonlinear least squares computer program which finds the horizontally-layered resistivity model whose response best fits the data (see Appendices A and B). The interpretative models used in this report include layers whose resistivities are either constant or transitional between adjacent constant-resistivity layers. A resistivity that varies smoothly with depth can closely approximate the increase in salinity with depth which is characteristic of the transition zone between fresh and saline water. The ability to include a transitional layer in the resistivity model is necessary for attempting to model the depth and thickness of the transition zone in the geohydrologic model.

The ability of the EM or Schlumberger technique to resolve the three parts of the geoelectric section can be demonstrated by first calculating theoretical responses to known models consisting of three layers and then interpreting these synthetic soundings with the least-squares program. The first layer represents fresh water saturated sediments. The second layer, which has a resistivity given by

$$\rho_2(z) = 1 / (1/\rho_1 + (1/\rho_3 - 1/\rho_1) * (z - d_1) / d_2)$$

where ρ_1 is the resistivity of layer 1,
 ρ_2 is the resistivity of layer 2,
 ρ_3 is the resistivity of layer 3,
* denotes multiplication,
 z is depth from the surface,
 d_1 is the thickness of layer 1, and
 d_2 is the thickness of layer 2.

(linear conductivity), represents the transition zone. The third layer represents seawater saturated sediments.

Table I shows the reduced chi-squared values (measuring the average misfit) and the model parameters for the best-fitting two-layer model found by the least-squares program for each of several synthetic data sets. The synthetic sounding data were calculated for three-layer models with a variety of values of d_2 (thickness of the transitional layer) with ρ_1 set at 500 ohm-m, ρ_3 set at 1 ohm-m, and d_1 set to 5 m. The results for the best-fitting three-layer models are not included in Table I because their reduced chi-squared values were very small and actually expressed more about the floating point accuracy of the computations than the relative model fits. Larger values for the two-layer models indicate the fit is expectedly poorer using the two-layer model rather than the three-layer model.

TABLE I. Two-layer models fitted to synthetic sounding data

	d2 = 15	10	5	4	3	2.5
EM red. chi-sq.	0.2861	.0754	.0075	.0038	.0016	.0009
DC red. chi-sq.	13.76	2.534	.1326	.0524	.0163	.0076
EM rho1 = 500	19.3	24.1	48.3	63.5	91.3	114.5
DC rho1 = 500	490.4	495.7	499.0	499.4	499.7	499.8
EM rho2 = 1	1.1	1.0	1.0	1.0	1.0	1.0
DC rho2 = 1	1.0	1.0	1.0	1.0	1.0	1.0
EM d1 = 5	12.0	10.0	7.5	7.0	6.5	6.25
lyr middle d1+d2/2	12.5	10.0	7.5	7.0	6.5	6.25
DC d1 = 5	5.2	5.1	5.05	5.03	5.02	5.01

These studies with synthetic sounding data show that transitional layers are detectable by surface electrical methods only if the transitional layer is thick compared to its depth and if the data error is sufficiently low. The larger the average data error, the thicker the transitional layer must be in order to be resolved. Noiseless EM or Schlumberger data can be used to resolve a transitional layer that is less than one-half as thick as its depth. Using Table I, if the average error is 0.08% for slingram data or about 2.5% for DC sounding data, then the transitional layer must be twice as thick as its depth to be resolved.

Another conclusion which can be drawn from Table I is that Schlumberger sounding is much better at resolving the true resistivity of the material above the transitional layer. If true for field data then meaningful estimates of the bulk conductivity (and therefore equivalent salinity) of the fresh water can be made from Schlumberger data.

The idea behind the use of the reduced chi-squared value as a measure of goodness-of-fit of a particular model to a data set is to assure the selection of a model with the least number of parameters for interpretation. The reduced chi-squared statistic is the ratio of the sum of squares of the differences between data and model responses (PHI) and the number of degrees of freedom in the data (DF), and is defined explicitly in Appendix B. As a model's complexity increases, both PHI and DF decrease. In order for the reduced chi-squared statistic to also decrease as a model's complexity increases, PHI must decrease faster than DF. The level of model complexity beyond which PHI no longer decreases faster than the degrees of freedom is defined as the simplest model for our purposes. Therefore, if we compare the reduced chi-squared values for fits of several different models (e.g. a two- and three-layer model) to a particular data set, the model with the lowest reduced chi-squared value should be chosen. More complexity in the model is not justified.

In particular, if a resistivity model which includes a transitional layer cannot fit the data better than a model without such a layer, then the inclusion of the transitional layer in the interpretational model is not justified and the simpler model should be chosen. The consequence of this choice is that the transitional layer known to be in the synthetic soundings is replaced with a fictitious abrupt change between two layers of constant resistivity in the interpretational model. Some quantitative information can still be obtained about the transition zone even though our interpretational techniques cannot resolve the zone explicitly. From Table I, we know that the abrupt change in model resistivity is located approximately at the middle of the transitional layer for slingram data and very near the top of the transitional layer for Schlumberger data.

It might be argued that if we know that a transitional layer exists from non-geophysical evidence, then we should only be using models in our interpretations with such a layer. Unfortunately, use of models with transitional layers to interpret actual sounding data shows that, in most cases, the interpreted transitional layer is meaninglessly thin. The effect of noise is to mask the existence of the transitional layer. Because the two-layer inversions require significantly less computation, they are far less expensive to obtain than three-layer inversions and are equally informative.

The data errors which might mask the existence of a transitional layer can be due to a number of causes. Major sources of error are departures of real earth layer boundaries from the horizontality and planarity assumed by the theoretical models used for interpretation, lateral changes in resistivity, pipes, fences, large metal structures, operational errors (mismeasured electrode or loop spacings), and natural noise. Even moderate data errors can mask the detail in the data that might be useable for resolving a transitional layer. The synthetic soundings were the simplest case possible containing only three layers and having only one layer above the transitional layer. It would be an even more difficult task to resolve a transitional layer below two or more layers.

Results of Electromagnetic sounding/profiling on Laura Island

A total of 196 stations were occupied along 12 lines across Laura in April 1984 (Figure 4). Three lines along which monitor wells were located were remeasured in October 1986. In both surveys, the height of the loops above sea level was assumed to be a constant 3 meters. The loops were held a constant 1 meter above the ground surface which was an average of 2 m above sea level. Ground surface elevations were not measured at each station.

The equipment was first calibrated by making sets of measurements at 51, 61 and 71 m separation over ground which is known to be highly resistive (a location in Hawaii Volcanoes National Park, HI which has resistivities in excess of 10,000 ohm-m to a depth of several hundred meters). The instrument gains may be calibrated by comparing the three sets of measurements to what one would theoretically expect to measure at these distances. The data set taken at 61 m is then used to reduce all field measurements (see Appendix A).

Using a computer program, all the data were inverted for the best-fitting two-layer and three-layer (with transitional layer) models. Without exception, the reduced chi-squared values for the three-layer models were larger than those for the two-layer models: The inclusion of a transitional layer is not justified. The parameters of the two-layer models for the 1984 and 1986 data sets are tabulated in Appendix A. Figure 5 is a contoured map of the depth below sea level to the geoelectric interface (the first model layer thickness minus the height of the loops above sea level) from the 1984 data.

The first geoelectric unit is about 15 m thick at its thickest on the eastern (lagoon) side, with a finger-shaped lobe running north beneath the island. This configuration is in general agreement with the configuration of hydraulic heads measured by Huxel (unpublished data, 1973) strongly suggesting that the first geoelectric unit corresponds to the fresh water lens.

The resistivities interpreted above and below the geoelectric interface appear related solely to the salinity of the saturating water. The resistivity of the material below the geoelectric interface (probably sea water-saturated coralline material) is between 0.5 and 1.3 ohm-m. The EM resistivity of the material above the geoelectric interface ranges from a few ohm-meters to values above the detection range (above 200 ohm-m). Most of the upper layer resistivity values are not well resolved by the data, and are unreliable. The poor resolution of the upper layer resistivity is of no consequence because it does not affect the resolution of the lower layer resistivity or the upper layer thickness.

Cultural contamination in the form of buried metallic pipes or other large metallic objects appeared to distort the data at two places on the profile labeled 'NS Line #1'. The two areas of distortion are the first four stations and stations 5400 to 6200. The distortion apparently makes the geoelectric interface appear deeper than it is in reality.

Comparison of the 1984 geophysical results with hydrologic data

Hamlin and Anthony (1987) monitored salinity at six locations on Laura (Figure 4) between September 1984 and September 1985. Unfortunately, salinity data are not available for the period of the geophysical survey work, so a direct comparison is not possible. In the following discussion, we will

attempt to extrapolate the hydrologic conditions in April 1984 from the record of conditions between September 1984 and September 1985.

Salinity data for the monitor period show that the lens was steadily thickening, i.e. the depth to the 500 mg/l reference isochlor was increasing. From April to September, 1985 the 500 mg/l isochlor moved about one meter deeper. Monthly rainfall for 1984 and 1985 show a similar linear increase between April and September of each year so it is reasonable to assume that the 500 mg/l data for 20 September 1984 is, at the most, one meter deeper than it would have been in April 1984, the time of the geophysical survey. Therefore, adding 1 m to depths interpreted from data obtained in April 1984 should approximate conditions in September 1984.

If we assume that the transition zone can be approximated by a linear change in salinity, then the geoelectric interface should represent a chloride content of about 9000 mg/l (50% seawater). Careful comparison of the two-layer EM interpretations and the September, 1984 chloride data shows that the geoelectric interface (plus 1 m) correlates with a chloride content of between 5400 and 14000 mg/l for holes D and E and less than 6800 mg/l for hole F (Figure 6). For monitor hole I at the northern end of the island, the geoelectric interface (plus 1 m) is at a depth which corresponds to a chloride content of less than 3000 mg/l (Figure 7). For monitor hole A, the geoelectric interface (plus 1 meter) is about 3 m below the single chloride determination of 750 mg/l. And for hole P, the geoelectric interface (plus 1 meter) is about 1 m below the deepest measuring interval which had a chloride content of 2540 mg/l in September, 1984.

In each comparison, the geoelectric interface is within the upper half of the transition zone, not at the transition zone midpoint as predicted by the linear salinity-increase model. Also the position of the interface does not consistently predict the same chloride content. This is not surprising; the geophysical measurements are averages over a subsurface region whose dimensions are controlled by the loop separation, whereas the wells are point measurements. We know that the isochlors are curved on the scale of the width of Laura island. Curvature and disruption of the lens on the scale of the slingram loop separation could result in interpreted depths which are shallower than the actual depths. The geophysically-averaged depths to the geoelectric interface can be expected to never be deeper than the midpoint of the transition zone.

Could the electromagnetic sounding be sensing or be confused by a resistivity contrast other than that between fresh and sea water? Cores (Hamlin and Anthony, 1986) from test holes D, E, and F (locations in Figure 4), show deposits of foraminiferal sand, Halimeda segments, and coral fragments. In addition, each section contains some silt. Without measuring the in situ resistivity of each of these sediment types, it is likely that silt probably has a lower resistivity than the other sediments. Comparing the sediment cross-section derived from the core data and the geophysical results for Line 6000N (Figure 6), it appears that the geoelectric interface does not correspond to the silt occurrences or changes in lithology. However, this set of data alone cannot answer the question definitively.

Comparison of the 1986 geophysical results with hydrologic data

The simultaneous measurement of three profiles of slingram, Schlumberger, and hydrologic data done in October 1986 allow a closer comparison of the results of these techniques than the previous data. The 1986 slingram data and two-layer interpretations are listed in Appendix A with data and results from the 1984 survey. In the 1986 survey, the geoelectric interface coincides with the depth to the deepest screened interval used for sampling at monitor holes D and F (Figure 6). The respective chloride contents (estimated from sample specific conductances measured by S. Anthony, written communication, 1986) are 4400 and 1300 mg/l. At monitor hole E, the geoelectric interface is 1.8 m below the deepest screened sampling interval which had an estimated chloride content of 600 mg/l. At monitor A, the geoelectric interface was 4.7 m below the deepest screened interval which had a measured chloride content of 190 mg/l. The sample from the deepest screened interval of monitor well I will not be used because of suspected contamination by water from higher in the lens (S. Anthony, oral communication, 1986). As in the earlier data, the areally-averaged estimates from slingram data of the depth to the geoelectric interface appear to place it within the upper half of the transition zone observed in monitor wells.

The 1986 survey results also allow comparison with the 1984 results to determine changes in the depth to the geoelectric interface, increases in the thickness of the transition zone (which was too thin to resolve in the earlier data, and whatever else might be detected. Without exception, the geoelectric interface is between 0.5 and 4.2 m deeper in October 1986 than in April 1984 (Figures 6 and 7). The EM-measured resistivity of the first geoelectric layer is also higher in the more recent measurements. Both of these geophysical conclusions support the idea that the fresh water lens has thickened between measurement periods. A thickened lens is also supported by significantly decreased chloride contents of all but the shallowest samples from the monitor wells (S. Anthony, written communication, 1986). As in the 1984 survey, no transitional layers were resolved and there was no perceptible change in the resistivity of the deepest geoelectric unit representing seawater-saturated sediments. The fact that the depth to the geoelectric interface has changed with time reaffirms the earlier conclusion that the slingram measurements are not sensitive to lithologic variations with depth, like those at Laura.

Several new pieces of information are available from the 1986 survey. Line 6000N was extended 305 m to the western edge of the island. Although the geoelectric interface is no more than 6 m below sea level anywhere along this extension, it appears to deepen again toward the west after having become dramatically shallower relative to the eastern side of the island (Figure 7). No further measurements were taken to either confirm, quantify or explain this observation.

For the first time on Majuro, Schlumberger soundings were obtained at monitor well locations A, D, E, F, and I (Appendix B). Transitional layers were not well resolved in this data set; however, the water table surface was clearly resolved in each sounding as an abrupt decrease in resistivity within a few tenths of a meter of sea level. The surface of the basement conductor is always above that determined from slingram measurements as we expect from the synthetic sounding study of transitional layer detectability done earlier. The resistivity of the fresh water material appears to have a resistivity of between 50 and 150 ohm-m. Using the salinity-resistivity relationship described earlier, these values suggest an average chloride content of between 120 and 360 mg/l for the water above the transition zone. Each sounding also indicated that the first few meters of the geoelectric layer that probably represents the water table was somewhat more conductive than the slightly deeper material within the fresh water-saturated portion of the lens. This might mean that the shallowest part of the fresh water lens was more saline than the deeper portions.

The 1986 survey also allows comparison of the slingram and Schlumberger techniques for the purpose of estimating various properties of the fresh water lens. Depth determinations to the basement conductor from Schlumberger data are more ambiguous than those from the slingram data because of the effects of the two or three layers above the interface of interest. However, the Schlumberger results appear to detect the water table directly. The synthetic sounding study discussed earlier showed that Schlumberger data can determine an average resistivity for the portion of the geoelectric model above the basement conductor. The slingram results are much less sensitive to this resistivity and are not sensitive at all to the shallow interface representing the water table. Finally, slingram is the only one of the two techniques which, as applied in Majuro, could determine the resistivity of the seawater-saturated sediments. This value is necessary as a reference to estimate crude average chloride contents from other resistivities in the geoelectric model.

Conclusions and Recommendations

As applied in Majuro, five-frequency slingram profiling using horizontal, coplanar loops works well for determining the depth to a point within the upper half (less than 4000 mg/l salinity) of the transition zone and the resistivity of the seawater-saturated coralline material when inverted with a program like MAROLOOPS_HP. Schlumberger sounding can determine the resistivity of the fresh water-saturated material within the lens and the depth to the water table from the ground surface. These quantities may be used to 1) estimate the average salinity of the fresh water portion of the lens and 2) estimate the configuration of the fresh water lens by mapping the depth to the

portion of the transition zone which contains less than 4000 mg/l salinity. The results compare well with chloride samples of wells through the lens, and do not appear to be disturbed by lithology variations. The quality of the interpretation using layered models seems quite good. It may be improved for this particular application by jointly inverting both slingram and Schlumberger data (Kauahikaua, 1986).

Appendix A: Slingram Data and Computer Interpretation

All loop-loop EM data were taken in the horizontal, coplanar loop mode (Parasnis, 1979) with the transmitter and receiver loops separated 61 m (200 ft). The in-phase or real (R) portion and the out-of-phase or imaginary (I) portion of the loop coupling at each of five frequencies - 222, 444, 888, 1777, 3555 Hz were measured. The data units are in percent of the coupling that would be observed in the absence of all conductive material. Note that the R measurement is actually equal to the real portion of the coupling minus 100 percent and that R values significantly greater than 35 are theoretically impossible for any horizontally-layered earth model and are indicative of distortion. Values are read on three different scales and therefore provide three different levels of precision. Values between plus and minus 4 percent can be read to the nearest 0.1 percent, values between plus and minus 20 percent can be read to the nearest 0.5 percent, and values between plus and minus 100 percent can be read to the nearest 2.5 percent.

The following is a complete list of all data recorded for this survey. Each line of this data set consists of one of the following two groups of information:

1. Line title
2. two pairs of station numbers and topographic elevations corresponding to the locations of each of the two loops used to obtain a particular set of data. The exact format is four fields of five in the order (from left to right) transmitter station number, elevation of transmitter, receiver station number, and elevation of receiver. Blanks for the elevation fields are treated as 'no data'. This is followed on the line by five pairs of in-phase and out-of-phase data values measured with the equipment. The exact format is 10 fields of five, or five pairs of two fields of five. Each pair is in the order (left to right) in-phase measurement and out-of-phase measurement. Each pair corresponds to one of five frequencies in the order (again left to right) 222, 444, 888, 1777, and 3555 Hertz.

The data from each field profile is headed by a line title and each measurement consists of one line with the station numbers, elevations and data. One unique measurement is denoted with the word 'CALIBRATION' in the first 11 columns of the line title and is followed with one data line consisting of values by which all following measurements are normalized.

The calibration equation is as follows:

$$A + iB = [(1+C/100) + iD/100] / [(1+E/100) + iF/100]$$

$$\text{corrected in-phase} = 100*(A-1)$$

$$\text{corrected out-of-phase} = 100*B$$

where C = in-phase field measurement,

D = out-of-phase field measurement,

E = in-phase calibration measurement, and

F = out-of-phase calibration measurement.

Data obtained at Laura, Majuro Atoll in April, 1984

CALIBRATION 200 1

		-15.0	-1.0-15.0	-0.3-15.0	+0.2-16.0	+1.5-14.5	+2.5
NS Line 1 ->N							
00	200	+16.0	0.0+13.0-12.5	-4.0-15.0-12.5	0.0	-2.5+10.0	
100	300	+16.5	-1.5+13.5-16.0	-4.0-26.0-16.0-17.0-17.5-18.0			
200	400	+15.0	-4.5+10.0-22.0	-9.0-31.0-25.0-24.0-29.0-27.0			
400	600	+16.5	-3.0+12.0-20.0	-7.0-28.0-24.0-16.0-25.0	-9.5		
600	800	+16.0	-3.0+11.5-17.5	-8.5-27.0-27.0-12.0-22.0	+1.0		
800	1000	+15.0	-9.0 +8.0-33.0-21.0-51.0-53.0-45.0-70.0-31.0				
1000	1200	+13.0-10.5	+5.0-34.0-24.0-52.0-58.0-46.0-75.0-30.0				
1200	1400	+17.0	-6.0+13.0-28.0-10.0-48.0-45.0-47.0-65.0-35.0				
1400	1600	+15.5	-9.0 +9.0-27.0-18.0-50.0-55.0-42.0-68.0-22.0				
1600	1800	+15.0-13.0	+5.0-37.0-27.0-52.0-61.0-39.0-72.0-17.0				
1800	2000	+16.0	-9.0 +9.0-31.0-17.5-47.0-51.0-38.0-63.0-18.0				
2000	2200	+18.5	-3.0+16.5-23.0	-3.0-41.0-35.0-41.0-53.0-27.0			
2200	2400	+15.0	-5.5+11.0-25.0	-9.0-39.0-37.0-35.0-50.0-25.0			
2400	2600	+15.0	-3.5+12.5-20.0	-5.0-34.0-30.0-32.0-42.0-23.0			
2600	2800	+15.0	-1.5+13.5-15.0	-1.0-29.0-23.0-27.0-32.0-17.5			
2800	3000	+18.0	+1.0+17.5-10.0	+6.5-22.0-10.5-18.0-19.0-10.0			
3000	3200	+15.0	+2.0+15.0	-7.5 +6.0-15.0	-8.0-13.0-13.0	-5.0	
3200	3400	+14.0	+3.0+15.0	-5.5 +8.0-12.0	-3.0-11.0	-8.0	-5.0
3400	3600	+14.5	+3.5+16.0	-3.5+12.0-11.0	+1.5-12.5	-2.5-11.0	
3600	3800	+13.0	+5.0+15.5	-2.0+12.0	-9.0 +2.5-10.0	-3.5	-8.0
3800	4000	+12.0	+4.0+14.5	-2.5+11.5	-9.5 +4.0-13.0	-1.0-14.5	
4000	4200	+11.0	+4.0+13.5	-2.0+10.5	-9.0 +3.0-12.5	-1.5-14.5	
4200	4400	+12.0	+4.5+14.0	-2.0+11.0	-8.5 +3.5-12.0	-1.0-12.5	
4400	4600	+11.5	+5.0+14.0	-1.0+11.5	-7.0 +4.5	-9.0 +1.0	-8.5
4600	4800	+11.0	+5.0+13.5	-0.5+12.0	-5.5 +5.5	-7.5 +2.5	-6.5
4800	5000	+11.0	+5.5+13.5	0.0+12.0	-5.0 +6.0	-7.0 +3.0	-6.0
5000	5200	+10.5	+5.0+13.0	0.0+12.0	-5.0 +6.0	-7.0 +3.5	-6.0
5200	5400	+11.0	+5.5+14.0	+0.5+12.5	-4.0 +6.5	-5.0 +5.0	-2.0
5400	5600	+12.5	+7.5+16.5	+3.5+16.0	-1.0+11.5	-1.5+11.0	+3.0
5600	5800	+14.5	+9.0+19.0	+5.0+19.5	+1.0+15.0	+0.5+16.0	+6.5
5800	6000	+14.0	+7.0+17.5	+3.0+17.0	-1.5+12.0	-1.5+12.0	+3.0
6000	6200	+11.5	+4.5+14.0	-2.0+11.0	-9.5 +2.5-12.5	-3.0-13.5	
6200	6400	+12.0	+3.5+14.0	-4.0+10.5-12.0	-1.0-16.0	-8.5-16.0	
6400	6600	+13.0	+3.5+15.0	-5.0 +9.5-14.5	-3.0-18.0-12.0-17.0		
6600	6800	+13.5	+1.5+14.0	-8.0 +7.5-18.0	-7.0-25.0-18.0-25.0		
6800	7000	+13.5	+1.5+15.0	-9.0 +7.5-19.0	-8.0-27.0-19.0-26.0		
7000	7200	+15.0	+1.0+16.0	-9.5 +7.5-23.0	-9.0-28.0-23.0-26.0		
7200	7400	+14.5	+1.0+15.0	-9.5 +6.0-23.0-10.0-26.0-24.0-24.0			
7400	7600	+15.0	+1.0+15.0	-9.5 +7.0-23.0	-9.5-26.0-23.0-24.0		
7600	7800	+14.5	+0.5+15.0	-9.5 +5.5-19.5-10.0-24.0-19.0-19.0			
7800	8000	+15.0	+1.0+15.0	-9.5 +6.0-23.0-10.0-26.0-23.0-23.0			
8000	8200	+14.5	-0.5+14.0-12.0	+4.0-26.0-14.0-28.0-28.0-24.0			
8200	8400	+15.5	-0.5+14.5-13.0	+3.0-28.0-15.0-30.0-31.0-25.0			
8400	8600	+15.5	-0.5+15.0-13.0	+3.0-28.0-15.0-30.0-31.0-25.0			
8600	8800	+15.0	-1.5+14.0-14.5	+1.0-29.0-18.0-32.0-34.0-27.0			
8800	9000	+16.0	0.0+15.5-12.0	+5.0-26.0-12.0-29.0-26.0-27.0			

9000	9200	+15.0	-1.0	+14.5	-13.0	+3.0	-28.0	-14.5	-31.0	-29.0	-30.0
9200	9400	+16.5	-1.0	+16.0	-13.5	+3.5	-29.0	-16.5	-33.0	-33.0	-31.0
9400	9600	+18.0	-1.0	+17.0	-15.0	+2.5	-32.0	-18.5	-35.0	-36.0	-30.0
9600	9800	+20.0	-3.0	+17.0	-20.0	-1.0	-38.0	-28.0	-38.0	-44.0	-29.0
EW Line 3600N ->W											
00	200	+12.5	+3.5	+14.5	-4.0	+10.0	-11.5	+0.5	-14.5	-5.0	-15.0
200	400	+11.5	+2.5	+12.0	-6.0	+6.0	-13.0	-5.0	-13.5	-10.0	-10.0
400	600	+13.5	+1.5	+13.5	-8.5	+5.0	-17.5	-8.5	-18.5	-16.5	-15.5
600	800	+14.0	+1.0	+13.5	-9.0	+5.0	-18.0	-9.0	-19.0	-16.0	-15.0
800	1000	+14.5	-0.5	+13.0	-12.5	+2.0	-25.0	-14.5	-26.0	-26.0	-22.0
1000	1200	+15.0	-7.0	+10.5	-27.0	-10.0	-45.0	-42.0	-46.0	-61.0	-35.0
1200	1400	+13.0	-9.5	+7.0	-32.0	-18.0	-47.0	-53.0	-44.0	-68.0	-28.0
EW Line 6000N ->W											
00	200	+11.0	+5.0	+13.0	-0.5	+11.5	-7.0	+6.0	-10.0	+3.5	-11.5
200	400	+10.5	+4.0	+13.0	-1.0	+11.0	-7.5	+4.5	-10.0	+0.5	-11.5
400	600	+10.5	+3.5	+12.5	-3.0	+9.5	-9.5	+1.5	-12.0	-2.5	-12.5
600	800	+11.0	+3.0	+12.5	-3.0	+8.5	-9.5	+1.0	-11.0	-3.0	-10.0
800	1000	+11.0	+3.0	+13.0	-4.0	+3.5	-10.0	-1.0	-12.0	-5.0	-11.0
1000	1200	+13.0	+3.0	+14.0	-5.0	+9.0	-12.0	-1.0	-14.0	-6.0	-13.0
1200	1400	+12.5	+1.0	+12.5	-8.0	+5.0	-16.5	-7.5	-17.0	-13.5	-15.5
1400	1600	+13.0	+0.5	+12.5	-9.0	+4.0	-17.5	-9.5	-18.0	-16.0	-15.5
1600	1800	+14.0	0.0	+13.5	-11.0	+3.0	-23.0	-12.0	-23.0	-19.0	-17.0
1800	2000	+14.5	-2.5	+12.0	-16.0	-2.5	-30.0	-22.0	-28.0	-33.0	-24.0
2000	2200	+16.5	-3.0	+14.0	-18.0	-2.5	-33.0	-27.0	-32.0	-38.0	-23.0
2200	2400	+17.0	-6.5	+12.5	-26.0	-8.5	-43.0	-38.0	-39.0	-53.0	-31.0
2400	2600	+18.0	-11.0	+10.0	-36.0	-18.0	-54.0	-55.0	-47.0	-71.0	-32.0
EW Line 8000N ->W											
00	200	+13.5	+1.5	+15.0	-7.5	+8.0	-17.5	-5.5	-24.0	-17.0	-24.0
200	400	+13.0	+2.0	+14.5	-5.5	+10.0	-14.0	-1.5	-18.5	-10.0	-19.0
400	600	+13.0	+2.5	+14.0	-6.0	+9.0	-14.0	-2.5	-17.0	-9.5	-16.5
600	800	+13.5	+2.0	+14.5	-7.0	+8.0	-15.0	-4.5	-16.5	-11.0	-14.0
800	1000	+13.5	0.0	+12.5	-10.0	+3.5	-19.0	-11.0	-20.0	-21.0	-11.5
1000	1200	+16.0	-0.5	+15.0	-12.0	+4.5	-24.0	-12.0	-26.0	-24.0	-19.0
1125	1325	+15.0	-2.0	+13.0	-14.5	-0.5	-28.0	-19.0	-28.0	-32.0	-23.0
EW Line 7400N ->W											
00	200	+16.5	+5.5	+20.0	-3.5	+16.5	-15.0	+3.0	-24.0	-8.0	-25.0
200	400	+15.5	+6.5	+18.5	-1.5	+15.5	-9.5	+6.0	-13.0	+2.0	-13.0
400	600	+14.5	+3.0	+16.0	-4.5	+11.5	-12.0	+0.5	-13.5	-4.5	-12.0
600	800	+20.0	+3.0	+22.0	-5.5	+16.5	-14.0	+4.5	-16.0	-2.0	-14.0
800	1000	+14.0	+1.0	+14.0	-9.0	+5.5	-17.5	-8.0	-18.0	-15.0	-15.5
1000	1200	+22.0	+3.0	+24.0	-8.0	+42.0	-23.0	+24.0	-25.0	+14.5	-19.0
1200	1400	+19.0	0.0	+18.5	-11.0	+8.0	-24.0	-8.0	-25.0	-17.0	-18.0
1400	1600	+25.0	0.0	+25.0	-12.0	+13.5	-27.0	-6.0	-29.0	-16.5	-24.0
1600	1800	+16.0	-2.5	+14.0	-15.5	-1.0	-30.0	-22.0	-30.0	-34.0	-25.0
EW Line 6400N ->E											
00	200	+15.0	-11.0	+7.0	-33.0	-22.0	-48.0	-51.0	-42.0	-65.0	-30.0
200	400	+15.0	-6.0	+9.5	-24.0	-10.0	-36.0	-35.0	-33.0	-45.0	-25.0
400	600	+16.5	-2.0	+14.0	-16.0	0.0	-29.0	-20.0	-28.0	-32.0	-23.0
600	800	+18.5	-1.0	+17.0	-13.5	+5.0	-26.0	-13.0	-27.0	-24.0	-22.0
800	1000	+13.5	0.0	+13.0	-10.5	+2.5	-23.0	-13.0	-23.0	-23.0	-17.0
1000	1200	+11.5	+1.0	+11.5	-8.0	+3.5	-16.5	-9.5	-17.0	-16.0	-13.5
1200	1400	+12.0	+3.0	+13.5	-5.0	+8.5	-12.0	-2.0	-14.0	-7.0	-12.5

1400	1600	+11.0	+3.5+13.0	-3.5	+9.0-10.0	-0.5-12.5	-5.5-11.0
1600	1800	+12.0	+4.0+14.5	-3.0+10.5	-10.0	+1.5-13.0	-3.5-13.0
1800	2000	+14.0	+5.5+17.5	-0.5+15.0	-8.0	+7.5-11.0	+4.0-11.5
2000	2200	+14.0	+3.5+16.0	-5.0+11.5	-14.0	0.0-19.0	-9.0-23.0
EW Line 9800N ->E							
00	200	+15.0	-0.5+14.0	-11.5	+4.0-24.0	-12.5-24.0	-23.0-19.0
200	400	+13.5	0.0+12.5	-11.0	+2.5-23.0	-12.0-23.0	-22.0-18.0
400	600	+14.0	-1.5+12.5	-13.0	+1.0-26.0	-16.0-28.0	-29.0-25.0
575	775	+16.0	-3.0+13.5	-16.5	-2.0-32.0	-24.0-33.0	-39.0-28.0
EW Line 4600N ->E							
00	-200	+17.0	-7.0+13.0	-30.0	-12.5-49.0	-49.0-45.0	-65.0-29.0
00	200	+46.0	-5.5+44.0	-28.0+21.0	-49.0	-12.5-50.0	-36.0-39.0
200	400	+41.0	+4.5+43.0	-7.5+36.0	-23.0+18.0	-26.0	+8.5-24.0
400	600	+13.0	+2.0+13.5	-7.0	+7.0-14.5	-5.0-15.0	-10.0-13.0
600	800	+16.5	+4.0+18.0	-4.0+13.0	-11.0	+3.5-13.0	-2.0-12.0
800	1000	+22.0	+4.5+24.0	-3.0+20.0	-10.5+10.5	-12.0	+6.0-10.5
1000	1200	+21.0	+4.5+24.0	-2.0+20.0	-9.0+12.5	-11.0	+8.5 -9.0
1200	1400	+28.0	+5.5+32.0	-1.0+29.0	-8.0+20.0	-10.5+17.0	-9.0
1400	1600	+10.5	+4.0+12.5	-2.5	+9.0 -8.5	+1.0-10.5	-2.5 -9.0
1600	1800	+11.0	+4.5+13.0	-1.0+11.5	-6.5	+5.0 -9.0	+2.5-10.0
1800	2000	+15.0	+4.5+17.5	-2.5+15.0	-10.5	+6.5-16.0	-1.0-23.0
EW Line 2900N ->E							
00	200	+15.0	-4.0+13.0	-24.0	-7.0-42.0	-37.0-42.0	-56.0-32.0
200	400	+13.0	-8.0	+9.0-28.0	-14.5-46.0	-48.0-43.0	-65.0-29.0
400	600	+15.0	-5.5+12.0	-25.0	-10.0-44.0	-39.0-47.0	-62.0-37.0
600	800	+14.0	-3.0+11.0	-17.0	-4.5-31.0	-26.0-30.0	-37.0-24.0
800	1000	+15.5	+1.0+15.5	-11.5	+4.0-25.0	-14.0-26.0	-25.0-23.0
1000	1200	+18.5	+1.0+18.0	-11.5	+6.5-26.0	-11.5-26.0	-23.0-23.0
EW Line 10200N ->E							
00	200	+17.5	+1.0+17.0	-11.0	+6.5-24.0	-9.0-25.0	-19.0-21.0
200	400	+17.0	-1.0+15.5	-13.5	+4.0-26.0	-14.0-29.0	-27.0-26.0
400	600	+18.5	-3.0+16.0	-18.0	-1.0-34.0	-25.0-34.0	-39.0-27.0
EW Line 5200N ->W							
00	200	+10.5	+5.0+13.5	0.0+12.0	-6.0	+6.0 -8.0	+3.5 -8.5
200	400	+9.0	+4.0+12.0	-1.0+10.0	-6.0	+3.5 -8.0	+1.0 -8.0
400	600	+10.5	+4.0+12.5	-2.0+10.0	-7.5	+3.0 -9.0	+0.5 -8.5
600	800	+14.0	+5.0+16.5	-1.0+14.0	-7.0	+7.0 -9.0	+4.0 -8.5
800	1000	+13.0	+4.0+15.0	-2.5+11.5	-9.5	+3.0-11.0	-1.0-11.0
1000	1200	+78.0	+9.5+85.0	+3.5+86.0	-7.0+75.0	-13.0+72.0	-13.5
1200	1400	+20.0	+4.5+22.0	-3.0+18.5	-10.0	+9.5-12.5	+5.0-12.0
1400	1600	+19.0	+2.5+20.0	-6.0+14.5	-14.5	+2.5-16.0	-4.0 -9.5
1600	1800	+22.0	+3.0+23.0	-6.5+17.0	-16.0	+3.5-17.5	-3.0-15.0
1800	2000	+16.5	+1.0+16.5	-9.5	+7.5-19.0	-7.5-23.0	-16.0-18.0
2000	2200	+15.5	-1.5+13.5	-14.5	0.0-29.0	-20.0-28.0	-30.0-23.0
2200	2400	+11.5	-13.5	+1.5-35.0	-29.0-48.0	-58.0-37.0	-68.0-24.0
NS Line 2 ->N							
200	00	+16.5	-7.5+11.0	-30.0	-14.0-48.0	-46.0-44.0	-62.0-33.0
400	200	+16.5	-9.0+10.5	-33.0	-16.5-50.0	-50.0-45.0	-67.0-32.0
600	400	+15.0	-8.0+10.0	-30.0	-14.0-48.0	-47.0-45.0	-63.0-32.0
800	600	+15.5	-6.5+10.5	-28.0	-12.0-45.0	-42.0-42.0	-58.0-32.0
1000	800	+16.0	-4.0+13.5	-24.0	-6.0-42.0	-36.0-43.0	-55.0-35.0
1200	1000	+14.0	-5.0+11.0	-25.0	-9.0-41.0	-38.0-41.0	-55.0-31.0

1400	1200	+16.0	-3.5+14.0-23.0	-5.0-40.0-35.0-41.0-52.0-35.0
1600	1400	+15.5	-4.0+13.0-24.0	-7.0-42.0-36.0-43.0-54.0-34.0
1800	1600	+16.0	-4.0+13.5-24.0	-5.5-42.0-35.0-43.0-54.0-34.0
2000	1800	+15.5	-4.0+13.0-23.0	-6.0-41.0-35.0-42.0-55.0-35.0
2200	2000	+16.0	-3.5+14.0-23.0	-4.5-40.0-34.0-41.0-52.0-33.0
2400	2200	+13.5	-7.5 +8.5-27.0-13.0-44.0-45.0-40.0-61.0-27.0	
2600	2400	+15.0	-6.5+11.0-26.0-10.5-44.0-42.0-42.0-58.0-30.0	
2800	2600	+15.0	-5.0+12.0-26.0	-8.5-44.0-41.0-44.0-59.0-33.0
3000	2800	+15.0	-5.5+11.5-26.0	-8.5-44.0-40.0-44.0-58.0-33.0
3200	3000	+15.0	-4.5+12.5-24.0	-7.0-43.0-37.0-44.0-57.0-35.0
3400	3200	+16.0	-4.5+13.0-25.0	-7.5-44.0-38.0-44.0-59.0-34.0
3600	3400	+15.5	-6.5+11.5-27.0-10.0-45.0-42.0-45.0-61.0-32.0	
3800	3600	+14.5	-7.5 +9.5-29.0-14.5-47.0-48.0-44.0-65.0-29.0	
4600	4800	+12.0-11.5	+3.0-34.0-26.0-48.0-55.0-39.0-68.0-26.0	
4800	5000	+12.0-10.0	+4.5-30.0-21.0-44.0-49.0-38.0-62.0-27.0	
5000	5200	+15.0	-2.5+12.5-17.0	-3.5-32.0-27.0-31.0-38.0-24.0
5200	5400	+14.5	-2.0+12.5-15.0	-1.5-29.0-22.0-29.0-33.0-24.0
5400	5600	+14.0	-1.0+12.0-13.5	-0.5-27.0-17.5-26.0-30.0-22.0
5600	5800	+15.5	-2.0+13.5-15.0	0.0-30.0-18.5-30.0-33.0-25.0
5800	6000	+14.5	-3.5+12.0-17.0	-4.5-32.0-27.0-31.0-37.0-24.0
6000	6200	+17.0	-3.5+14.0-21.0	-3.5-36.0-30.0-35.0-44.0-28.0
6200	6400	+17.5	-6.0+13.0-26.0	-9.0-43.0-38.0-40.0-54.0-31.0
6400	6600	+15.0	-9.5 +8.0-33.0-19.0-49.0-51.0-43.0-67.0-30.0	
6600	6800	+16.5	-8.0+11.0-29.0-12.5-44.0-43.0-41.0-58.0-31.0	
6800	7000	+15.5	-5.0+11.0-24.0	-8.5-38.0-33.0-35.0-48.0-28.0
7000	7200	+16.0	-4.5+12.0-23.0	-7.0-36.0-32.0-35.0-45.0-27.0
7200	7400	+15.5	-3.5+12.5-18.5	-5.0-35.0-28.0-28.0-41.0-26.0
7400	7600	+15.0	-7.0 +9.0-26.0-12.0-38.0-38.0-36.0-51.0-28.0	
7600	7800	+17.0	-7.0+11.0-28.0-12.0-41.0-39.0-37.0-52.0-27.0	
7800	8000	+15.0-11.0	+6.0-34.0-23.0-48.0-50.0-39.0-64.0-27.0	
8000	8200	+16.5-10.5	+8.5-34.0-20.0-49.0-52.0-42.0-65.0-28.0	
8200	8400	+15.0-12.0	+6.0-35.0-24.0-50.0-55.0-42.0-69.0-29.0	
8400	8600	+16.0	-8.5 +9.0-30.0-15.0-44.0-48.0-37.0-56.0-26.0	
8600	8800	+14.0-10.5	+6.5-32.0-19.0-48.0-50.0-43.0-67.0-32.0	
8800	9000	+16.0	-6.0+11.5-25.0	-9.0-38.0-35.0-36.0-48.0-28.0
9000	9200	+15.0	-5.5+11.0-24.0	-8.0-37.0-33.0-35.0-45.0-27.0
9200	9400	+16.0	-4.0+13.0-19.0	-4.0-34.0-27.0-33.0-40.0-27.0
9400	9600	+17.0	-3.5+14.5-17.5	-1.5-33.0-23.0-31.0-35.0-26.0
9600	9800	+15.0	-4.0+12.0-18.0	-2.5-33.0-27.0-31.0-38.0-26.0
9800	10000	+16.5	-3.0+14.0-16.5	-1.5-31.0-23.0-31.0-36.0-25.0
10000	10200	+18.0	-2.0+16.5-16.0	+1.5-31.0-22.0-32.0-33.0-26.0
10200	10400	+17.0	-3.0+14.5-17.0	-1.5-32.0-24.0-32.0-36.0-26.0
10400	10600	+17.0	-3.5+13.5-19.5	-4.0-35.0-29.0-34.0-42.0-26.0
10600	10800	+10.5-12.0	+0.5-33.0-26.0-41.0-51.0-31.0-59.0-20.0	
10800	11000	+18.0	-5.0+14.0-24.0	-6.0-38.0-31.0-36.0-47.0-29.0
11000	11200	+15.5	-4.5+12.0-21.0	-6.0-35.0-30.0-34.0-44.0-28.0
11200	11400	+16.5	-3.5+13.0-18.5	-3.5-34.0-26.0-33.0-40.0-27.0
11400	11600	+16.0	-2.5+14.0-16.0	-1.0-31.0-22.0-31.0-35.0-26.0
11600	11800	+16.5	-0.5+15.0-13.5	+2.5-28.0-15.5-29.0-30.0-25.0
11800	12000	+17.0	0.0+16.0-12.0	+5.0-26.0-14.0-27.0-25.0-24.0
12000	12200	+17.0	0.0+16.0-12.5	+5.0-26.0-12.0-27.0-25.0-24.0
12200	12400	+18.0	0.0+17.0-12.5	+5.0-26.0-12.5-28.0-26.0-26.0

12400	12600	+16.5	-2.0	+15.0	-15.0	+2.0	-29.0	-16.5	-31.0	-32.0	-29.0
12600	12800	+17.5	-2.5	+15.5	-17.0	0.0	-34.0	-23.0	-30.0	-41.0	-30.0
12800	13000	+18.0	-6.0	+14.0	-25.0	-5.0	-40.0	-32.0	-40.0	-50.0	-32.0
13000	13200	+17.0	-7.5	+11.5	-28.0	-11.0	-44.0	-43.0	-42.0	-60.0	-30.0
13200	13400	+18.0	-9.5	+10.5	-31.0	-15.0	-48.0	-47.0	-43.0	-63.0	-29.0

Data obtained at Laura, Majuro Atoll on 22 October, 1986

CALIBRATION 200 1

		+1.9	-2.0	+1.8	-0.9	+2.0	+0.3	+0.7	+1.4	+2.8	+3.0
REPEAT LINE	5000	->W									
0	200	+17.0	+6.5	+25.0	+0.8	+23.0	-5.5	+17.0	-10.0	+12.5	-12.0
200	400	+19.0	+5.0	+24.0	+0.2	+22.0	-6.0	+15.0	-10.0	+11.0	-10.0
400	600	+18.0	+4.5	+23.0	-1.3	+18.5	-8.5	+11.5	-12.0	+6.5	-11.5
600	800	+18.0	+4.5	+22.0	-1.7	+18.0	-8.0	+9.5	-10.0	+4.0	-7.0
800	1000	+19.0	+4.5	+23.0	-2.4	+18.5	-9.5	+10.0	-12.5	+5.0	-10.5
1000	1200	+19.0	+4.0	+23.0	-3.2	+17.0	-10.5	+8.0	-14.0	+2.5	-12.0
1200	1400	+21.0	+2.6	+23.0	-6.0	+15.5	-14.0	+3.8	-17.0	-3.4	-14.0
1400	1600	+21.0	+2.3	+23.0	-7.5	+14.0	-16.5	+0.4	-19.0	-6.5	-15.0
1600	1800	+22.0	+1.9	+23.0	-8.5	+13.0	-17.5	-2.8	-22.0	-9.0	-15.0
1800	2000	+21.0	-0.8	+21.0	-14.0	+7.5	-26.0	-12.5	-28.0	-22.0	-22.0
2000	2200	+24.0	-0.9	+24.0	-15.0	+8.0	-29.0	-14.5	-30.0	-25.0	-22.0
2200	2400	+25.0	-2.2	+24.0	-18.5	+5.0	-35.0	-22.0	-37.0	-33.0	-28.0
2400	2600	+22.0	-9.5	+14.5	-33.0	-13.0	-49.0	-48.0	-45.0	-58.0	-29.0
2600	2800	+24.0	-11.0	+15.5	-35.0	-15.0	-50.0	-49.0	-42.0	-46.0	-24.0
2800	3000	+26.0	-10.0	+18.0	-34.0	-12.0	-51.0	-49.0	-43.0	-59.0	-23.0
3000	3200	+26.0	-9.5	+18.0	-33.0	-11.0	-49.0	-45.0	-43.0	-53.0	-25.0
3200	3400	+23.0	-7.5	+17.0	-29.0	-9.5	-45.0	-43.0	-39.0	-50.0	-23.0
3400	3600	+23.0	-6.0	+18.5	-28.0	-7.0	-45.0	-41.0	-40.0	-49.0	-25.0

REPEAT LINE 8000 ->W

0	200	+21.0	+2.3	+23.0	-7.0	+15.5	-17.0	+1.8	-24.0	-9.0	-22.0
200	400	+18.5	+3.5	+23.0	-4.0	+17.0	-12.5	+7.0	-18.0	-1.5	-20.0
400	600	+18.0	+3.5	+22.0	-4.0	+17.0	-12.0	+7.0	-16.0	-0.1	-15.5
600	800	+19.0	+3.0	+22.0	-5.0	+14.5	-13.5	+2.9	-16.0	-3.5	-13.0
800	1000	+20.0	+1.7	+23.0	-8.0	+13.0	-16.0	-1.1	-19.5	-8.0	-15.0
1000	1200	+23.0	+1.0	+23.0	-10.0	+12.5	-21.0	-4.5	-24.0	-13.0	-18.5
1200	1400	+25.0	-0.8	+25.0	-14.0	+10.0	-28.0	-10.5	-30.0	-21.0	-23.0

REPEAT LINE 3600 ->W

0	200	+21.0	+5.3	+25.0	-1.6	+20.0	-9.0	+11.5	+13.0	+6.5	-12.5
200	400	+18.0	+5.0	+22.0	-1.6	+15.0	-6.0	+4.0	-2.2	-2.6	+12.0
400	600	+20.0	+2.8	+23.0	-6.8	+15.0	-14.0	+2.5	-17.0	-3.5	-13.0

Interpretation and Tabulated Results

Interpretation was done with the aid of computer program MARQLOOPS_HP, an enhanced, Hewlett-Packard 9826 BASIC 4.0 version of program MARQLOOPS (Anderson, 1979b), which finds the best-fitting, horizontally-layered earth model for a given loop-loop EM profile data set. Input to the program consists of the data set, the number of layers, and a first guess at the resistivities and thicknesses of those layers. Layers may have constant or transitional resistivities. A transitional resistivity may vary linearly in either resistivity or conductivity and is approximated as a set of ten thin layers having appropriate resistivities (Mundry and Zschau, 1983). In addition, the program can automatically adjust the model for possible errors in loop spacing by varying the loop spacing as if it were another model parameter.

The results of interpreting the EM profiling data using program MARQLOOPS_HP are tabulated here under the following headings:

STN	Station number, in feet along profile.
RCHISQ	Reduced chi-squared value for the model-data fit. Locally large values indicate either a noisy data set or a geologic situation which departs significantly from the two-layer horizontally-layered model assumed here, e.g. wide transition zone or more than two geoelectric layers.
RHO1(OHM-M)	Resistivity of the first geoelectric unit in ohm-m.
RHO2(OHM-M)	Resistivity of the second geoelectric unit in ohm-m.
D1(M)	Thickness of the first geoelectric unit, in meters. Note that this distance is measured from the plane containing the source and receiver loops to the interface between the first and second layers of this model.

stn		1984 rchisq	rho1	rho2	d1
NS Line 1 ->N					
400	600	27.9	500	0.6	11.7
600	800	101.2	500	0.5	12.4
800	1000	1.58	7.9	1.0	5.6
1000	1200	0.81	5.8	1.0	5.9
1200	1400	0.49	8.2	1.1	5.9
1400	1600	13	189.6	1.1	4.3
1600	1800	10.9	500	0.9	4.4
1800	2000	14.4	155.2	0.9	5.0
2000	2200	0.58	133.9	1.1	5.9
2200	2400	1.16	43.8	0.9	7.4
2400	2600	0.69	86.4	0.9	8.5
2600	2800	4.7	500	0.9	10.0
2800	3000	11.6	500	0.8	12.5
3000	3200	21.5	500	0.7	14.2
3200	3400	12.1	500	0.8	15.6
3400	3600	0.45	95.1	0.8	16.7
3600	3800	1.86	500	0.9	16.5
3800	4000	0.30	38.5	0.9	18.1
4000	4200	0.01	38.2	0.9	18.5
4200	4400	0.24	50.8	0.9	18.2
4400	4600	0.13	102.8	0.9	18.8
4600	4800	0.23	150.1	0.9	19.7
4800	5000	0.21	186.6	0.9	19.8
5000	5200	0.34	131.0	0.9	20.3
5200	5400	1.7	500	0.8	20.6
5400	5600	9.6	500	1.0	22.1
5600	5800	17.2	500	1.0	24.6
5800	6000	8.4	500	0.9	22.4
6000	6200	0.04	53.7	0.9	17.4
6200	6400	0.4	54.2	1.0	15.6
6400	6600	0.06	66.2	1.0	14.3
6600	6800	1.3	21.7	1.0	13.8
6800	7000	1.9	20.6	1.0	13.3
7000	7200	0.94	24.7	1.0	11.7
7200	7400	0.90	32.1	1.0	11.8
7400	7600	1.1	31.1	1.0	11.8
7600	7800	1.7	49.9	0.9	12.7
7800	8000	0.99	35.0	1.0	11.8
8000	8200	1.4	32.6	1.0	11.1
8200	8400	2.2	31.4	1.0	10.4
8400	8600	1.9	32.2	1.0	10.3
8600	8800	1.5	22.5	1.0	10.3
8800	9000	1.0	20.6	1.0	11.5
9000	9200	1.4	15.0	0.9	11.7
9200	9400	0.58	15.8	1.0	10.4
9400	9600	1.3	19.0	1.0	9.2
9600	9800	0.63	24.0	1.0	7.3

1986

EW Line 3600N ->W						rchisq	rho1	rho2	d1
0	200	0.11	44.1	0.9	16.8	0.46	126.1	1.0	19.0
200	400	0.51	500	0.8	16.0				
400	600	0.07	99.7	0.8	13.8	0.70	500	0.9	16.7
600	800	0.50	98.1	0.8	13.8				
800	1000	0.97	34.6	0.9	11.8				
1000	1200	2.2	6.9	1.0	7.5				
1200	1400	2.6	16.2	1.0	5.4				

EW Line 6000N ->W						rchisq	rho1	rho2	d1
0	200	0.68	41.8	0.8	20.3	1.3	78.2	1.2	20.8
200	400	0.22	49.5	0.9	19.4	0.31	116.0	1.0	20.8
400	600	0.40	47.6	0.8	18.5	0.73	107.7	1.0	20.1
600	800	0.35	74.3	0.8	18.4	1.3	500	1.0	19.1
800	1000	3.8	61.2	0.7	18.3	0.45	230.2	1.0	19.2
1000	1200	0.23	61.2	0.8	16.6	0.59	181.1	0.9	18.6
1200	1400	0.33	55.0	0.8	15.0	0.22	277.4	0.9	16.9
1400	1600	0.23	68.3	0.8	14.3	0.55	481.7	0.9	15.9
1600	1800	4.2	58.6	0.8	12.8	2.3	500	0.9	15.0
1800	2000	1.2	29.1	0.9	10.6	1.1	166.7	0.9	13.0
2000	2200	1.5	63.6	0.9	8.8	1.68	500	1.0	11.6
2200	2400	1.3	13.6	0.9	7.1	3.59	117.8	1.0	10.2
2400	2600	2.3	7.6	0.9	4.8	7.33	10.7	0.9	9.0
2600	2800					9.81	500	0.9	7.1
2800	3000					9.34	500	0.9	6.8
3000	3200					8.57	500	0.9	7.2
3200	3400					10.56	500	0.9	8.2
3400	3600					9.04	500	1.0	8.2

EW Line 8000N ->W						rchisq	rho1	rho2	d1
0	200	1.1	24.2	1.0	13.7	0.74	45.7	1.0	15.9
200	400	0.85	33.0	0.9	15.4	0.49	41.7	1.0	18.5
400	600	0.35	43.4	0.9	15.5	0.43	78.2	1.0	18.5
600	800	0.33	85.5	0.8	14.9	0.41	500	0.9	17.1
800	1000	8.2	500	0.9	12.5	1.14	500	0.9	15.8
1000	1200	2.0	75.9	0.9	11.3	0.83	324.6	0.9	14.2
1125	1325	0.67	37.4	0.9	10.6				
1200	1400					1.60	159.7	1.0	12.2

EW Line 7400N ->W						rchisq	rho1	rho2	d1
0	200	0.90	27.2	1.2	13.0				
200	400	1.2	60.4	1.0	16.6				
400	600	0.31	88.6	0.8	16.1				
600	800	0.29	70.0	0.9	14.6				
800	1000	0.16	73.6	0.8	14.1				
1000	1200	138	29.7	1.3	12.4				
1200	1400	3.6	58.4	0.9	11.7				
1400	1600	1.7	30.8	0.9	10.2				
1600	1800	0.57	29.7	0.9	10.0				

EW Line 6400N ->E						rchisq	rho1	rho2	d1
0	200	2.77	10.0	0.9	6.4				
200	400	1.39	26.3	0.8	8.6				
400	600	0.31	39.0	0.9	10.3				
600	800	0.68	36.8	0.9	11.0				
800	1000	1.7	138.2	0.9	12.2				

1000	1200	0.32	154.3	0.8	14.6
1200	1400	0.33	75.0	0.8	16.4
1400	1600	0.25	99.7	0.9	17.1
1600	1800	0.11	57.8	0.9	17.2
1800	2000	0.39	56.9	0.9	18.0
2000	2200	0.29	23.9	1.0	15.5
EW Line 9800N ->E					
0	200	1.5	61.5	0.9	11.9
200	400	2.2	59.8	0.9	12.6
400	600	0.93	23.2	0.9	11.7
575	775	0.61	20.9	0.9	9.5
EW Line 4600N ->E					
0	-200	2.3	500	1.1	4.5
0	200	3.7	11.9	1.0	3.6
200	400	2.5	29.6	1.0	10.0
400	600	0.48	85.4	0.8	15.5
600	800	0.14	81.4	0.8	16.2
800	1000	0.31	88.3	0.8	16.1
1000	1200	0.69	86.0	0.8	17.0
1200	1400	0.58	84.5	0.9	16.3
1400	1600	0.35	105.8	0.8	18.3
1600	1800	0.22	54.1	0.8	20.1
1800	2000	0.48	21.3	0.9	17.5
EW Line 2900N ->E					
0	200	0.57	14.2	1.1	6.8
200	400	0.81	18.8	1.0	5.7
400	600	5.4	10.0	1.1	6.6
600	800	0.88	33.5	0.9	10.0
800	1000	0.61	37.4	0.9	11.3
1000	1200	1.2	38.0	0.9	11.0
EW Line 10200N ->E					
0	200	1.9	36.8	0.9	11.9
200	400	0.55	22.2	0.9	11.2
400	600	0.40	27.2	1.0	8.6
EW Line 5200N ->W					
0	200	0.23	70.2	0.9	20.1
200	400	0.34	80.0	0.8	20.3
400	600	0.41	77.0	0.8	19.6
600	800	0.21	87.4	0.8	18.8
800	1000	0.12	70.7	0.8	17.8
1000	1200	2.7	39.8	1.1	11.1
1200	1400	0.27	58.7	0.8	16.5
1400	1600	2.7	500	0.8	14.8
1600	1800	0.58	66.3	0.9	13.8
1800	2000	1.47	53.7	0.9	12.8
2000	2200	1.76	36.0	0.9	10.6
2200	2400	1.08	28.5	0.8	5.7
NS Line 2 ->N					
200	0	2.9	10.0	0.9	6.3
400	200	2.9	10.0	0.9	5.6
600	400	2.9	10.0	1.0	6.2
800	600	1.8	10.4	0.9	7.0

1000	800	0.88	10.0	1.0	7.5
1200	1000	1.11	13.3	1.0	7.4
1400	1200	1.02	10.2	1.0	7.9
1600	1400	1.4	10.2	1.0	7.5
1800	1600	1.2	10.6	1.0	7.3
2000	1800	0.70	10.0	1.0	7.8
2200	2000	0.55	12.9	1.0	7.4
2400	2200	1.12	34.2	1.0	6.1
2600	2400	1.02	16.3	1.0	6.4
2800	2600	1.2	11.3	1.1	6.6
3000	2800	1.9	10.5	1.0	6.9
3200	3000	2.3	10.0	1.0	7.5
3400	3200	0.82	10.1	1.1	6.8
3600	3400	1.5	11.2	1.0	6.3
3800	3600	0.78	18.1	1.0	5.5
4600	4800	0.81	15.9	0.9	6.0
4800	5000	0.52	15.0	0.9	7.0
5000	5200	1.2	45.0	0.9	9.3
5200	5400	0.78	32.5	0.9	10.5
5400	5600	1.26	40.7	0.9	11.2
5600	5800	1.93	27.0	0.9	10.3
5800	6000	2.2	35.1	0.9	9.6
6000	6200	0.38	23.6	1.0	8.2
6200	6400	0.48	13.7	0.9	6.9
6400	6600	1.0	10.0	0.9	5.8
6600	6800	0.70	11.4	0.9	6.8
6800	7000	0.88	18.2	0.9	8.3
7000	7200	0.70	21.8	0.9	8.4
7200	7400	5.7	31.4	0.9	9.2
7400	7600	0.54	15.7	0.8	8.2
7600	7800	0.92	20.0	0.9	7.2
7800	8000	1.96	13.5	0.8	6.1
8000	8200	1.04	14.1	0.9	5.3
8200	8400	1.04	10.0	0.9	5.7
8400	8600	5.13	28.7	0.9	6.3
8600	8800	13.2	10.0	0.9	6.9
8800	9000	0.67	17.8	0.9	8.1
9000	9200	1.78	19.6	0.9	8.5
9200	9400	0.53	22.1	0.9	9.2
9400	9600	1.47	24.2	0.9	9.6
9600	9800	2.12	26.1	0.9	9.5
9800	10000	0.43	31.1	0.9	9.6
10000	10200	1.3	28.6	0.9	9.4
10200	10400	0.78	26.5	0.9	9.4
10400	10600	0.56	31.6	0.9	8.4
10600	10800	2.4	500	0.7	7.0
10800	11000	0.57	17.1	0.9	8.0
11000	11200	0.05	19.1	0.9	8.9
11200	11400	0.69	22.7	0.9	9.1
11400	11600	0.60	25.6	0.9	9.9
11600	11800	1.22	28.9	0.9	10.6
11800	12000	0.71	31.2	0.9	11.1

12000	12200	1.02	29.2	0.9	11.2
12200	12400	0.49	24.2	0.9	11.1
12400	12600	0.89	16.6	0.9	10.9
12600	12800	7.0	19.8	1.0	9.2
12800	13000	1.49	11.6	0.9	7.8
13000	13200	0.73	14.7	1.0	6.2
13200	13400	0.89	14.0	0.9	5.5

APPENDIX B: Schlumberger Sounding Data and Computer Interpretations

A Schlumberger or Wenner resistivity sounding consists of a series of apparent resistivity measurements taken at several different electrode positions created by expanding four electrodes symmetrically about a central point (two on each side), preferably along a straight line. Electric current is forced into the ground through the outer two electrodes (current electrodes) and the voltage produced by that current is measured between the inner two electrodes (potential electrodes). Larger current electrode separations generally force deeper current penetration; thus, it is possible to influence the depth of investigation by varying the current electrode separation. For the Schlumberger electrode array, the potential electrodes are placed no farther apart than one-fifth the separation between the current electrodes.

Anomalies due to local lateral inhomogeneities can sometimes be recognized by moving either the potential electrodes or the current electrodes between readings, but not both at the same time. In practice, the potential electrodes in the Schlumberger array are moved once for every four or five current electrode moves. Apparent resistivity values obtained for the same current electrode separation with two different potential electrode separations are almost always slightly different due to small inhomogeneities around the electrodes and/or the use of homogeneous earth potential variations to reduce real, nonhomogeneous earth potential variations; these differences must be removed to give an unbroken data set for quantitative interpretation. The differences are removed by holding a data segment, made with a particular potential electrode separation, fixed and shifting the remaining segments up or down so that the end points match adjacent segments. There are many conventions for deciding to which base segment the rest will be shifted. For most sounding data sets, all segments are shifted to the segment measured with the largest potential electrode spacing.

Computer program MARQDCLAG_HP, an enhanced Hewlett-Packard 9826 BASIC version of MARQDCLAG (Anderson, 1979a), offers an automatic means by which sounding data sets, like those obtained in the course of this study, can be inverted to their best-fitting horizontally-layered model parameters - resistivities and thickness. The layers in the model may either have a uniform resistivity or a resistivity which varies from the resistivity of the layer above it to the resistivity of the layer below. The resistivity can be selected to vary linearly in either resistivity or conductivity. A transitional layer is approximated by a set of ten thin layers having appropriate resistivities (Mundry and Zschau, 1983). Approximate matching can be done by manually comparing the sounding data to theoretical curves in a standard album; however, the computer inversion offers several advantages, including speed, automation, and estimation of parameter resolution.

MARQDCLAG_HP automatically minimizes the following quantity:

$$PHI = \sum_{i=1}^N \left[\frac{y_i - f(x_i)}{e_i} \right]^2$$

where N is the number of data in the sounding data set,

x_i is the i^{th} current electrode spacing,
 y_i is the measured apparent resistivity measured at x_i ,
 e_i is the apparent resistivity measurement error
 (default = $y_i / 100$), and
 $f(x)$ is the theoretical apparent resistivity calculated from the earth model.

Along with the sounding data set, the program requires a starting guess of all model parameters.

The number of layers cannot be automatically varied by the program. A common practice is to invert each sounding data set for several models, each having a different number of layers. The best-fitting model is chosen to be the one which minimizes the following quantity, called the reduced chi-squared statistic:

$$REDUCED\ CHI-SQUARED = PHI / (N - 1 - K)$$

where K is the number of parameters in the model being fit to the data. In general applications, $K = 2 * m - 1$ where m is the number of layers in the theoretical model and * denotes multiplication.

During the inversions of the sounding data sets, the natural logarithm of the model parameters, rather than the parameters themselves, were manipulated to avoid the possibility of negative resistivities or thicknesses and to more accurately reflect the logarithmic resolution of these values. The values and their error estimates are converted back to normal units before being output by the program. A detailed description of the headings and identifying terms used in the program output listed in this Appendix follows:

X electrode spacing equal to half the distance between the two current electrodes, meters,

OBSERVED shifted observed apparent resistivity values, ohm-meters,

MARQUARDT STATISTICS: Laura86 at well A

	X	OBSERVED	PREDICTED	%RESIDUALS	WEIGHT FN
1	+1.5240E+00	+1.9852E+02	+2.1876E+02	-1.0194E+01	+6.0285E-05
2	+1.9812E+00	+2.2222E+02	+2.0990E+02	+5.5427E+00	+4.8114E-03
3	+2.4384E+00	+1.9812E+02	+1.9842E+02	-1.4938E-01	+6.0528E-03
4	+3.0480E+00	+1.7592E+02	+1.8052E+02	-2.6131E+00	+7.6770E-03
5	+3.9624E+00	+1.4944E+02	+1.5233E+02	-1.9350E+00	+1.0639E-02
6	+4.8768E+00	+1.2335E+02	+1.2684E+02	-2.8303E+00	+1.5614E-02
7	+6.0960E+00	+1.0095E+02	+1.0031E+02	+6.3326E-01	+2.3312E-02
8	+7.6200E+00	+7.7755E+01	+7.8344E+01	-7.5732E-01	+3.9297E-02
9	+9.1440E+00	+6.7700E+01	+6.4931E+01	+4.0895E+00	+5.1838E-02
10	+1.2192E+01	+5.3500E+01	+5.0449E+01	+5.7030E+00	+8.3007E-02
11	+1.5240E+01	+4.2600E+01	+4.1847E+01	+1.7684E+00	+1.3092E-01
12	+1.9812E+01	+3.1400E+01	+3.1778E+01	-1.2052E+00	+2.4097E-01
13	+2.4384E+01	+2.2400E+01	+2.3453E+01	-4.7028E+00	+4.7351E-01
14	+3.0480E+01	+1.4900E+01	+1.5069E+01	-1.1314E+00	+1.0702E+00
15	+3.9624E+01	+7.4000E+00	+7.6122E+00	-2.8682E+00	+4.3387E+00
16	+4.8768E+01	+5.0000E+00	+4.1384E+00	+1.7231E+01	+9.5035E+00

CORRELATION MATRIX:

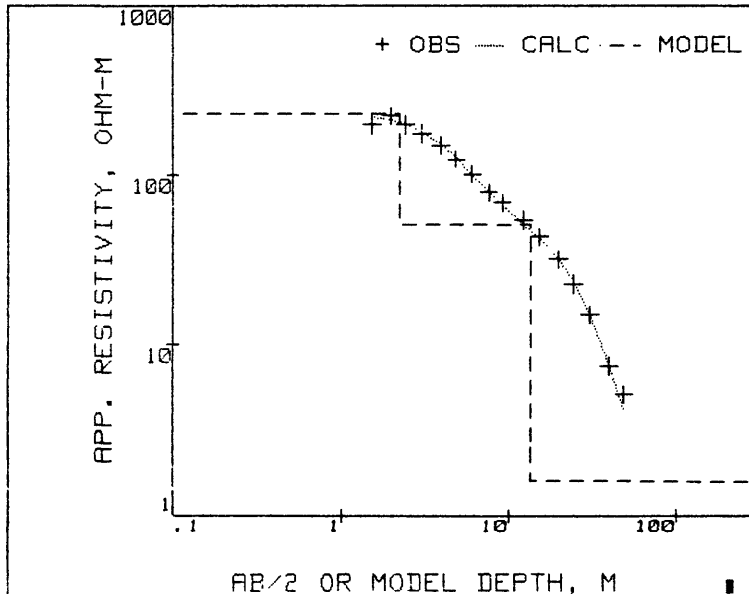
	1	2	3	4	5
1	+1.00	+0.46	+0.22	-0.77	-0.25
2	+0.46	+1.00	+0.64	-0.80	-0.83
3	+0.22	+0.64	+1.00	-0.44	-0.91
4	-0.77	-0.80	-0.44	+1.00	+0.55
5	-0.25	-0.83	-0.91	+0.55	+1.00

REDUCED CHI-SQUARED=43.37
PHI=433.7

DCLAG: ***** END ***** Laura86 at well A
COORDINATES: 0 0
ELEVATION : 1.8 METER
AZIMUTH : S80W

RESISTIVITY			THICKNESS			DEPTH	ELEV
159.9	227.9	325.0	1.4	2.2	3.6	0.0	1.8
30.1	50.4	84.2	7.5	11.3	16.8	2.2	-0.4
.1	1.5	21.8				13.5	-11.7

Laura86 at well A



MARQUARDT STATISTICS: Laura86 at well D

	X	OBSERVED	PREDICTED	%RESIDUALS	WEIGHT FN
1	+1.5240E+00	+2.5149E+02	+2.7674E+02	-1.0039E+01	+7.0350E-03
2	+1.9812E+00	+2.7651E+02	+2.6633E+02	+3.6814E+00	+5.8199E-03
3	+2.4384E+00	+2.5339E+02	+2.5255E+02	+3.3027E-01	+6.9302E-03
4	+3.0480E+00	+2.4417E+02	+2.3053E+02	+5.5843E+00	+7.4635E-03
5	+3.9624E+00	+2.0248E+02	+1.9463E+02	+3.8795E+00	+1.0853E-02
6	+4.8768E+00	+1.6446E+02	+1.6093E+02	+2.1458E+00	+1.6451E-02
7	+6.0960E+00	+1.2404E+02	+1.2467E+02	-5.0643E-01	+2.8919E-02
8	+7.6200E+00	+9.1579E+01	+9.3949E+01	-2.5879E+00	+5.3055E-02
9	+9.1440E+00	+7.2126E+01	+7.5346E+01	-4.4635E+00	+8.5533E-02
10	+1.2192E+01	+5.8737E+01	+5.7056E+01	+2.8612E+00	+1.2897E-01
11	+1.5240E+01	+4.8000E+01	+4.8358E+01	-7.4616E-01	+1.9312E-01
12	+1.9812E+01	+3.7800E+01	+3.9449E+01	-4.3627E+00	+3.1141E-01
13	+2.4384E+01	+3.2500E+01	+3.1693E+01	+2.4843E+00	+4.2126E-01
14	+3.0480E+01	+2.4300E+01	+2.2639E+01	+6.8369E+00	+7.5354E-01
15	+3.9624E+01	+1.2700E+01	+1.2587E+01	+8.9310E-01	+2.7588E+00
16	+4.8768E+01	+6.3000E+00	+6.5193E+00	-3.4817E+00	+1.1211E+01

CORRELATION MATRIX:

	1	2	4	5	6	7
1	+1.00	+0.43	-0.25	-0.68	-0.30	+0.30
2	+0.43	+1.00	-0.74	-0.86	-0.85	+0.84
4	-0.25	-0.74	+1.00	+0.56	+0.97	-0.97
5	-0.68	-0.86	+0.56	+1.00	+0.66	-0.65
6	-0.30	-0.85	+0.97	+0.66	+1.00	-1.00
7	+0.30	+0.84	-0.97	-0.65	-1.00	+1.00

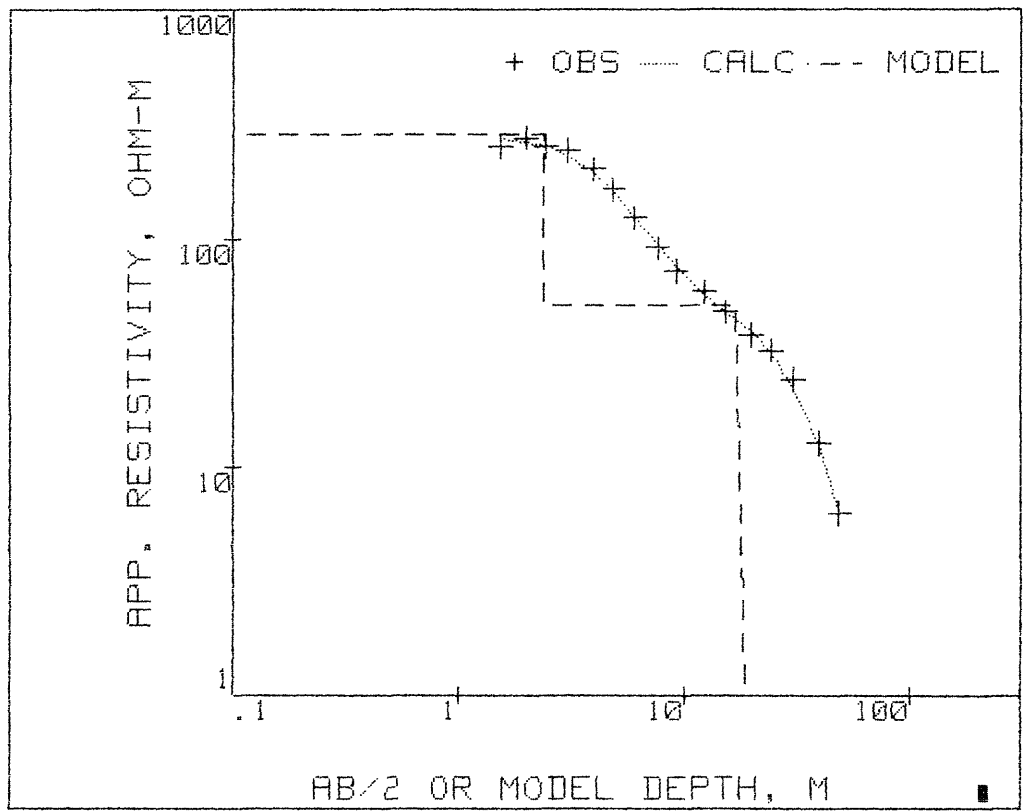
REDUCED CHI-SQUARED=31.75
 PHI=285.78

DCLAG: ***** END ***** Laura86 at well D
 COORDINATES: 0 0
 ELEVATION : 2.1 METER
 AZIMUTH : S86W

RESISTIVITY			THICKNESS			DEPTH	ELEV
242.6	287.3	340.1	1.8	2.4	3.1	0.0	2.1
30.1	51.0	86.6	0.0	14.6		2.4	-1.3
*****	-2.0*****		0.0	1.7		17.0	-14.9
0.0	0.0					18.7	-16.6

MODEL HAS LAYERS WHOSE RESISTIVITIES ARE TRANSITIONAL BETWEEN ADJACENT LAYERS:
 RESISTIVITY OF -1 SIGNIFIES LINEAR RESISTIVITY
 RESISTIVITY OF -2 SIGNIFIES LIENAR CONDUCTIVITY

Laura86 at well D



	X	OBSERVED	PREDICTED	%RESIDUALS	WEIGHT FN
1	+1.5240E+00	+1.3251E+02	+1.5280E+02	-1.5314E+01	+9.1245E-05
2	+1.9812E+00	+1.4796E+02	+1.4244E+02	+3.7279E+00	+4.5742E-02
3	+2.4384E+00	+1.2932E+02	+1.3053E+02	-9.3461E-01	+5.9878E-02
4	+3.0480E+00	+1.1260E+02	+1.1444E+02	-1.6350E+00	+7.8985E-02
5	+3.9624E+00	+9.0383E+01	+9.3576E+01	-3.5330E+00	+1.2258E-01
6	+4.8768E+00	+7.7872E+01	+7.8295E+01	-5.4274E-01	+1.6513E-01
7	+6.0960E+00	+6.7404E+01	+6.5294E+01	+3.1311E+00	+2.2040E-01
8	+7.6200E+00	+5.8340E+01	+5.6437E+01	+3.2630E+00	+2.9421E-01
9	+9.1440E+00	+5.2213E+01	+5.1690E+01	+1.0007E+00	+3.6731E-01
10	+1.2192E+01	+4.6723E+01	+4.6543E+01	+3.8665E-01	+4.5869E-01
11	+1.5240E+01	+4.2638E+01	+4.2852E+01	-5.0167E-01	+5.5080E-01
12	+1.9812E+01	+3.6000E+01	+3.7425E+01	-3.9577E+00	+7.7265E-01
13	+2.4384E+01	+3.0900E+01	+3.1889E+01	-3.2022E+00	+1.0488E+00
14	+3.0480E+01	+2.5800E+01	+2.4963E+01	+3.2447E+00	+1.5044E+00
15	+3.9624E+01	+1.6700E+01	+1.6757E+01	-3.3905E-01	+3.5905E+00
16	+4.8768E+01	+1.1600E+01	+1.1382E+01	+1.8805E+00	+7.4417E+00
17	+6.0960E+01	+2.4000E+00	+7.4282E+00	-2.0951E+02	+2.7816E-01

CORRELATION MATRIX:

	1	2	3	4	5
1	+1.00	+0.47	+0.23	-0.83	-0.26
2	+0.47	+1.00	+0.62	-0.74	-0.75
3	+0.23	+0.62	+1.00	-0.40	-0.95
4	-0.83	-0.74	-0.40	+1.00	+0.47
5	-0.26	-0.75	-0.95	+0.47	+1.00

REDUCED CHI-SQUARED=14.8

PHI=162.77

DCLAG: ***** END *****

Laura86 at well E

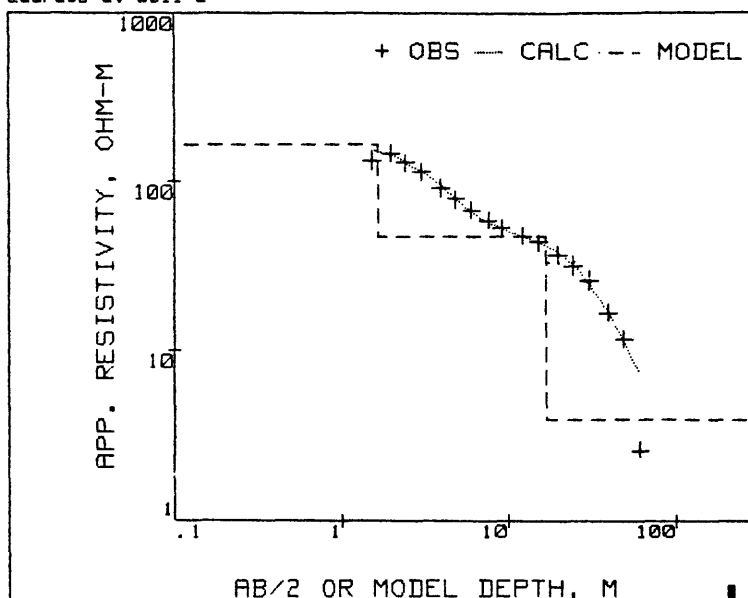
COORDINATES: 0 0

ELEVATION : 1.8 METER

AZIMUTH : S67W

RESISTIVITY			THICKNESS			DEPTH	ELEV
143.0	165.2	190.9	1.4	1.7	2.0	0.0	1.8
42.3	46.9	52.0	12.5	15.3	18.7	1.7	.1
1.3	3.8	10.7				16.9	-15.1

Laura86 at well E



MARQUARDT STATISTICS: Laura86 at well F

	X	OBSERVED	PREDICTED	%RESIDUALS	WEIGHT FN
1	+1.5240E+00	+2.9226E+02	+2.7548E+02	+5.7410E+00	+8.2163E-04
2	+1.9812E+00	+2.6468E+02	+2.5101E+02	+5.1629E+00	+1.0018E-03
3	+2.4384E+00	+2.0930E+02	+2.2344E+02	-6.7591E+00	+1.6021E-03
4	+3.0480E+00	+1.7263E+02	+1.8725E+02	-8.4691E+00	+2.3549E-03
5	+3.9624E+00	+1.4429E+02	+1.4256E+02	+1.2005E+00	+3.3708E-03
6	+4.8768E+00	+1.1725E+02	+1.1217E+02	+4.3348E+00	+5.1049E-03
7	+6.0960E+00	+9.0749E+01	+8.8932E+01	+2.0022E+00	+8.5216E-03
8	+7.6200E+00	+7.5606E+01	+7.5331E+01	+3.6326E-01	+1.2277E-02
9	+9.1440E+00	+6.6088E+01	+6.8666E+01	-3.9012E+00	+1.6068E-02
10	+1.2192E+01	+5.7002E+01	+5.9435E+01	-4.2686E+00	+2.1599E-02
11	+1.5240E+01	+4.2400E+01	+4.9826E+01	-1.7515E+01	+3.9037E-02
12	+1.9812E+01	+3.7100E+01	+3.5505E+01	+4.3000E+00	+5.0987E-02
13	+2.4384E+01	+2.7200E+01	+2.3773E+01	+1.2598E+01	+9.4856E-02
14	+3.0480E+01	+1.1700E+01	+1.3221E+01	-1.2996E+01	+5.1266E-01
15	+3.9624E+01	+4.8000E+00	+5.4013E+00	-1.2528E+01	+3.0459E+00
16	+4.8768E+01	+2.4000E+00	+2.5071E+00	-4.4606E+00	+1.2184E+01

CORRELATION MATRIX:

	1	2	3	4	5	7
1	+1.00	+0.62	-0.57	-0.19	-0.81	+0.58
2	+0.62	+1.00	-0.98	-0.45	-0.93	+0.98
3	-0.57	-0.98	+1.00	+0.55	+0.87	-1.00
4	-0.19	-0.45	+0.55	+1.00	+0.35	-0.57
5	-0.81	-0.93	+0.87	+0.35	+1.00	-0.88
7	+0.58	+0.98	-1.00	-0.57	-0.88	+1.00

REDUCED CHI-SQUARED=118.3

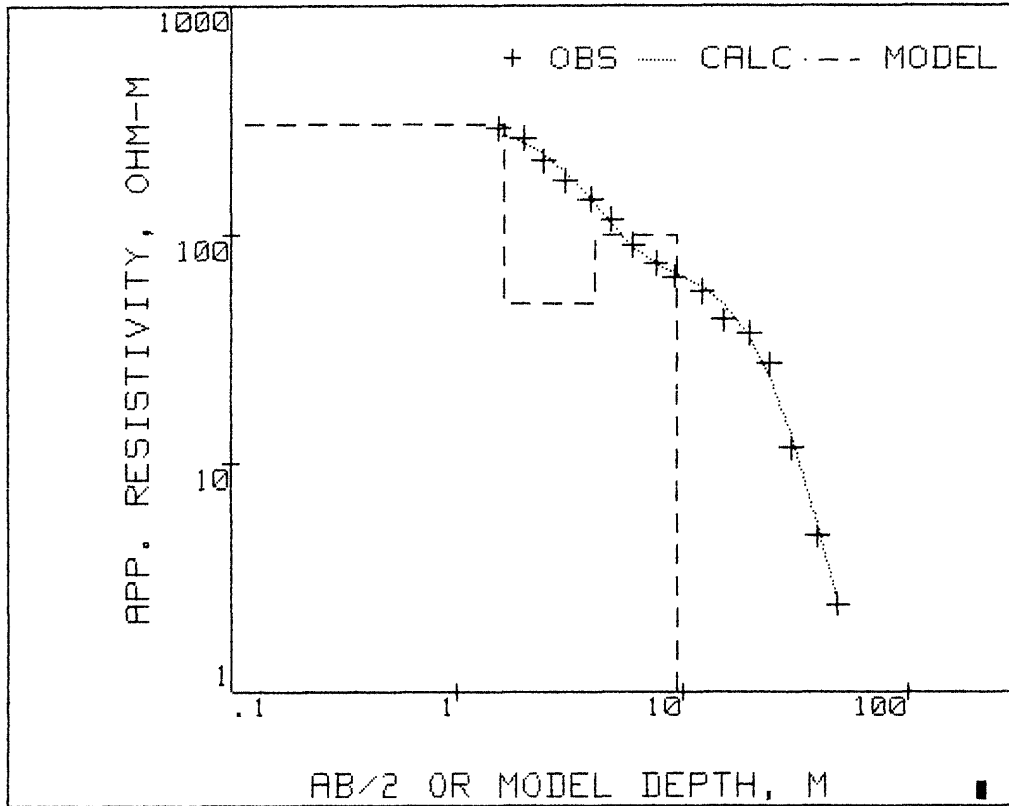
PHI=1064.5

DCLAG: ***** END *****
 COORDINATES: 0 0
 ELEVATION : 1.5 METER
 AZIMUTH : S70W

Laura86 at well F

RESISTIVITY			THICKNESS			DEPTH	ELEV
73.8	305.4	1263.7	.1	1.6	23.0	0.0	1.5
0.0	50.8	127104.0*****		2.5*****		1.6	-1
0.0	100.0		0.0	5.3		4.1	-2.6
0.0	1.0	303.3				9.4	-7.9

Laura86 at well F



MARQUARDT STATISTICS: Laura86 at well I

	X	OBSERVED	PREDICTED	%RESIDUALS	WEIGHT FN
1	+1.5240E+00	+3.3728E+02	+3.5111E+02	-4.1003E+00	+2.0448E-03
2	+1.8288E+00	+3.3480E+02	+3.4159E+02	-2.0270E+00	+2.0752E-03
3	+2.2860E+00	+3.3642E+02	+3.2361E+02	+3.8080E+00	+2.0553E-03
4	+2.7432E+00	+3.0538E+02	+3.0257E+02	+9.1749E-01	+2.4944E-03
5	+3.0480E+00	+2.9557E+02	+2.8770E+02	+2.6618E+00	+2.6627E-03
6	+3.9624E+00	+2.4404E+02	+2.4382E+02	+9.0665E-02	+3.9057E-03
7	+4.8768E+00	+2.1138E+02	+2.0667E+02	+2.2265E+00	+5.2060E-03
8	+6.0960E+00	+1.6783E+02	+1.7127E+02	-2.0479E+00	+8.2581E-03
9	+7.6200E+00	+1.4035E+02	+1.4502E+02	-3.3323E+00	+1.1810E-02
10	+9.1440E+00	+1.2870E+02	+1.2985E+02	-8.8866E-01	+1.4043E-02
11	+1.2192E+01	+1.1135E+02	+1.0957E+02	+1.5983E+00	+1.8761E-02
12	+1.5240E+01	+9.4318E+01	+9.0615E+01	+3.9269E+00	+2.6148E-02
13	+1.9812E+01	+6.1657E+01	+6.3433E+01	-2.8796E+00	+6.1188E-02
14	+2.4384E+01	+4.6824E+01	+4.1678E+01	+1.0989E+01	+1.0609E-01
15	+3.0480E+01	+2.0700E+01	+2.2553E+01	-8.9537E+00	+5.4286E-01
16	+3.9624E+01	+8.8000E+00	+8.8154E+00	-1.7543E-01	+3.0038E+00
17	+4.8768E+01	+4.2000E+00	+3.9237E+00	+6.5786E+00	+1.3187E+01

CORRELATION MATRIX:

	1	2	3	4	5	7
1	+1.00	+0.66	-0.65	-0.22	-0.76	+0.65
2	+0.66	+1.00	-1.00	-0.48	-0.98	+1.00
3	-0.65	-1.00	+1.00	+0.51	+0.97	-1.00
4	-0.22	-0.48	+0.51	+1.00	+0.42	-0.51
5	-0.76	-0.98	+0.97	+0.42	+1.00	-0.97
7	+0.65	+1.00	-1.00	-0.51	-0.97	+1.00

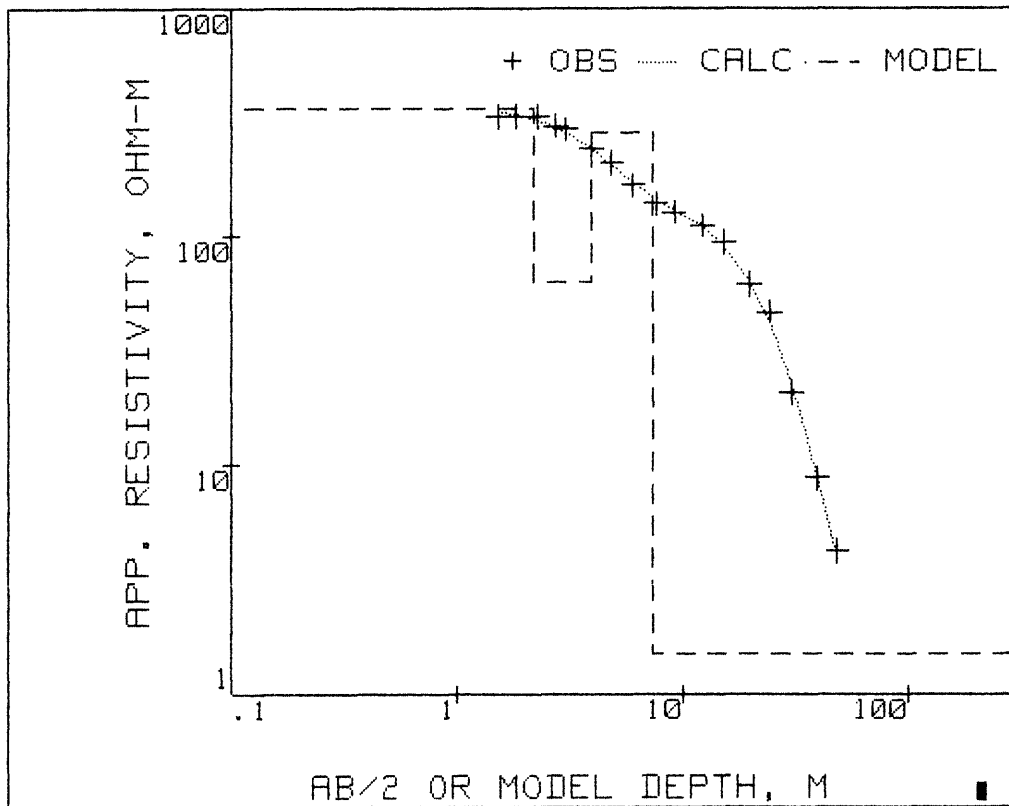
REDUCED CHI-SQUARED=33.49
 PHI=334.91

DCLAG: ***** END *****
 COORDINATES: 0 0
 ELEVATION : 2.1 METER
 AZIMUTH : N75W

Laura86 at well I

RESISTIVITY			THICKNESS			DEPTH	ELEV
263.9	367.0	510.3	.3	2.2	13.7	0.0	2.1
0.0	62.7		*****	1.8*****		2.2	-1.1
0.0	283.5		0.0	3.4		4.0	-1.9
.2	1.5	9.9				7.4	-5.3

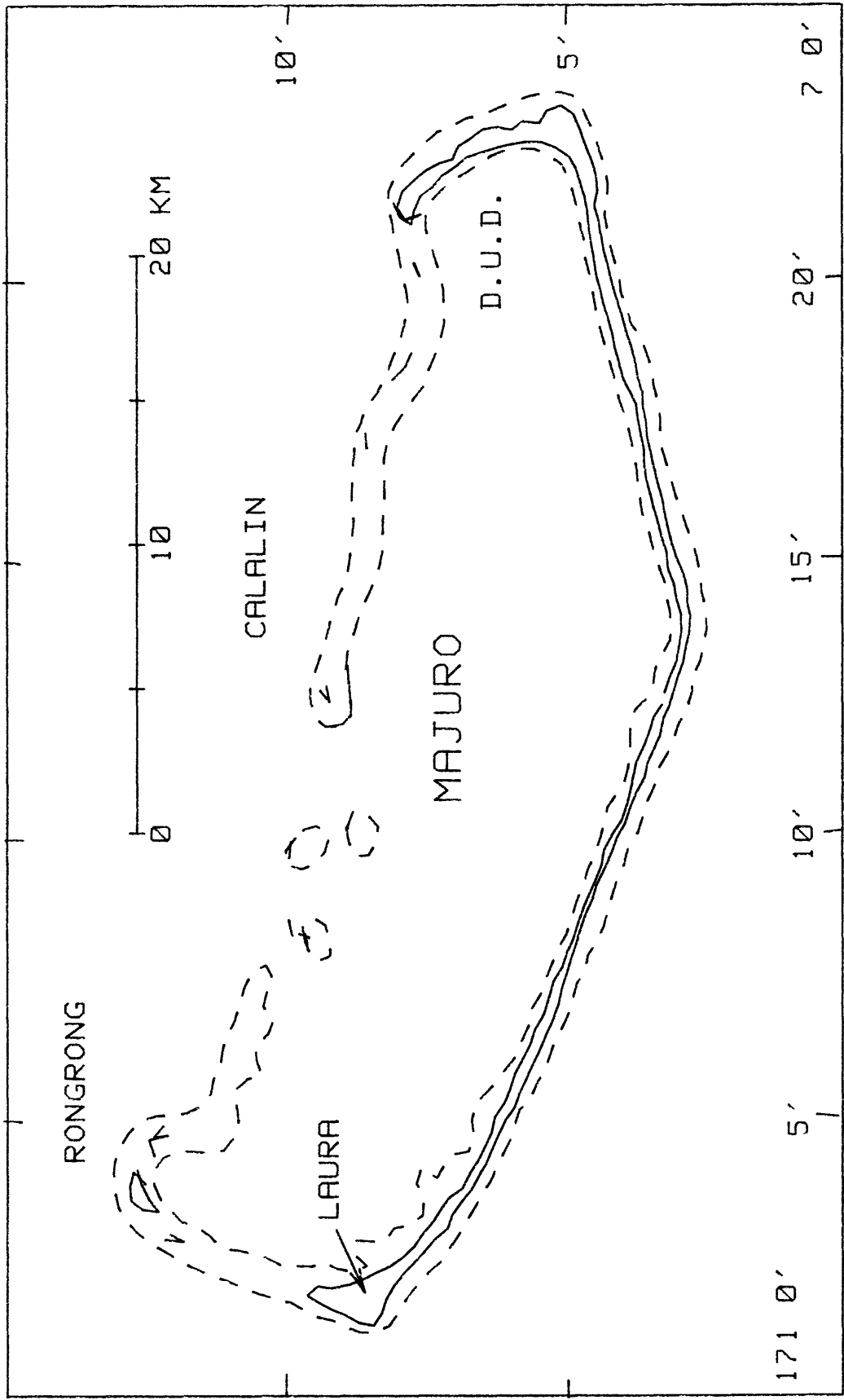
Laura86 at well I



List of Figures

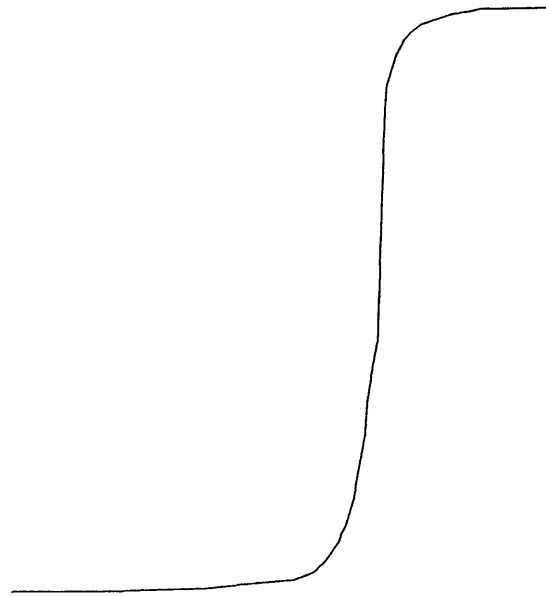
- Figure 1. A map of Majuro Atoll, Republic of the Marshall Islands, showing the area called Laura.
- Figure 2. A comparison of salinity versus depth and geoelectric model resistivity versus depth graphs for conditions expected in Laura. Model resistivity depth profiles are shown for both a two-layer model and a three-layer model with an intermediate layer having a transitional resistivity.
- Figure 3. Examples of the theoretical response of the five-frequency EM system to a three-layer model containing different thicknesses of a transitional layer. The real portion of the response is plotted horizontally and the quadrature portion is plotted vertically. Each response consists of five pairs of numbers - one at each of five frequencies. The point representing data at 222 Hz is plotted at the upper right and the point representing data at 3555 Hz is plotted at the lower left of each response curve.
- Figure 4. A map of Laura Island showing the names and locations of each of the profiles. The profiles are named for the point at which they intersect NS Line #1. Also shown are the names and locations of six monitor well sites.
- Figure 5. A map of Laura Island showing contoured depths of the geoelectric interface in meters below sea level from the April 1984 data. Also shown are the names and locations of the six monitor well sites.
- Figure 6. A cross-section along Line 6000N showing the lithology, the screened intervals from which chloride samples were taken in the three monitor well, chloride contents of samples obtained on Sept. 1984, Sept. 1985 (Hamlin and Anthony, 1986), and Oct. 1986 (S. Anthony, written communication, 1986) and the geoelectric interface interpreted from data taken in early April, 1984 and October, 1986.
- Figure 7. A cross-section along Line 8000N showing the screened intervals from which chloride samples were taken in the monitor wells, chloride contents of samples obtained on Sept. 1984, Sept. 1985 (Hamlin and Anthony, 1987), and

Oct. 1986 (S. Anthony, written communication, 1986) and the geoelectric interface interpreted from data taken in April, 1984 and October, 1986.

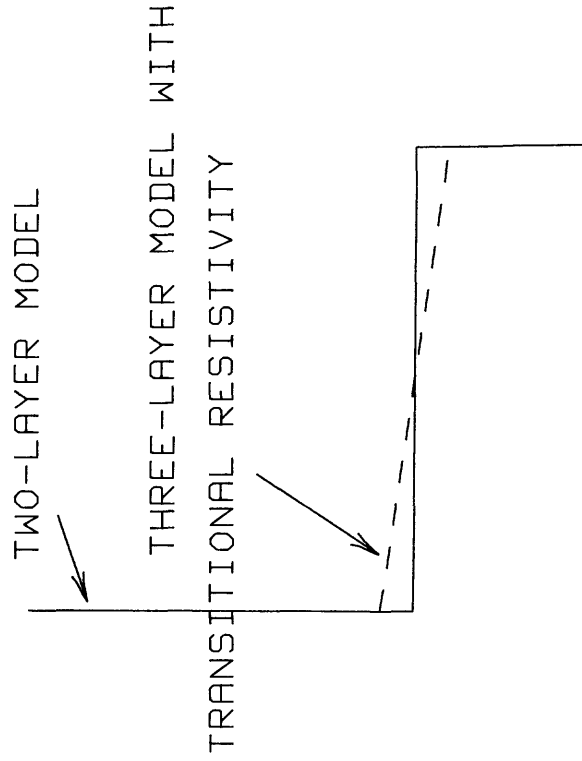


HYDROLOGIC MODEL

GEOELECTRICAL MODEL

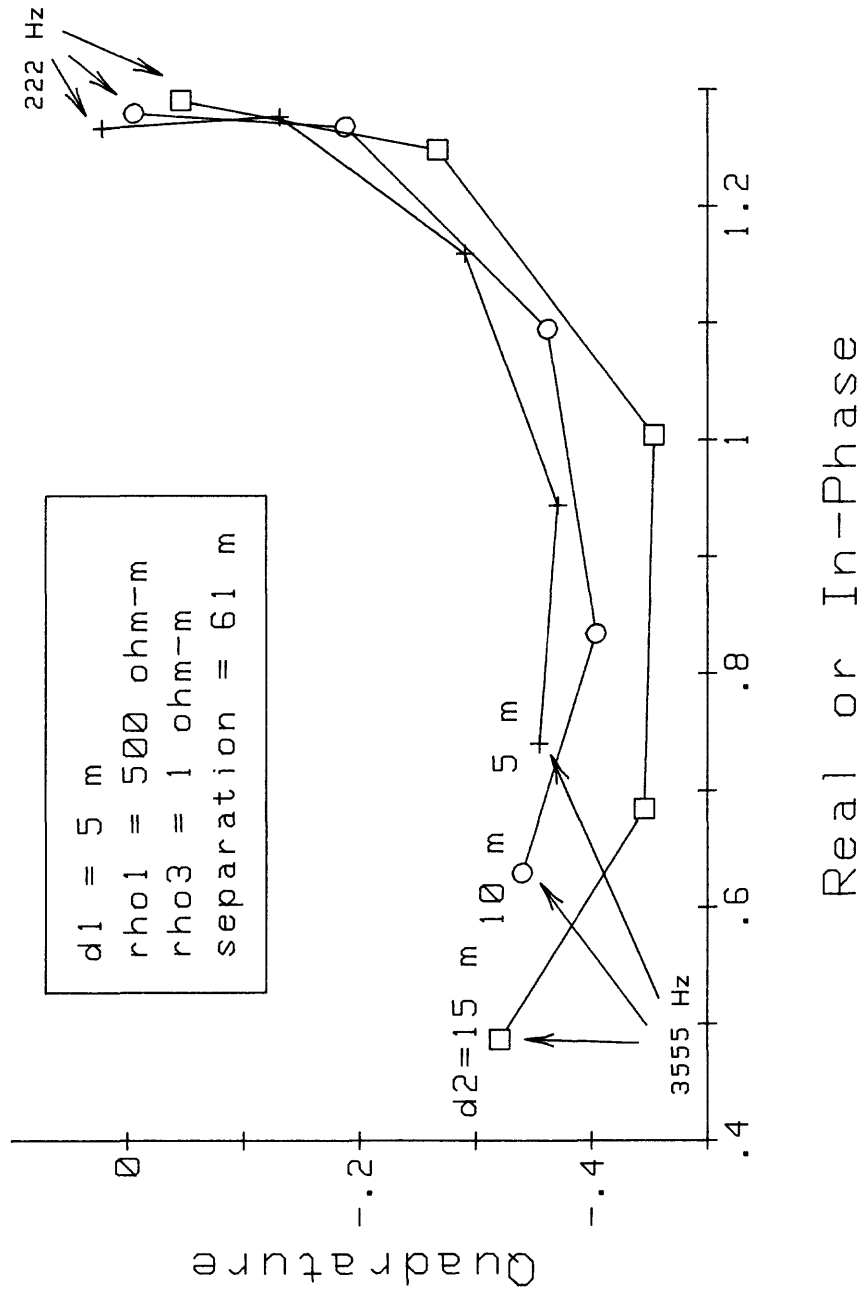


0 1000 2000
CHLORIDE CONCENTRATION (mg/l)

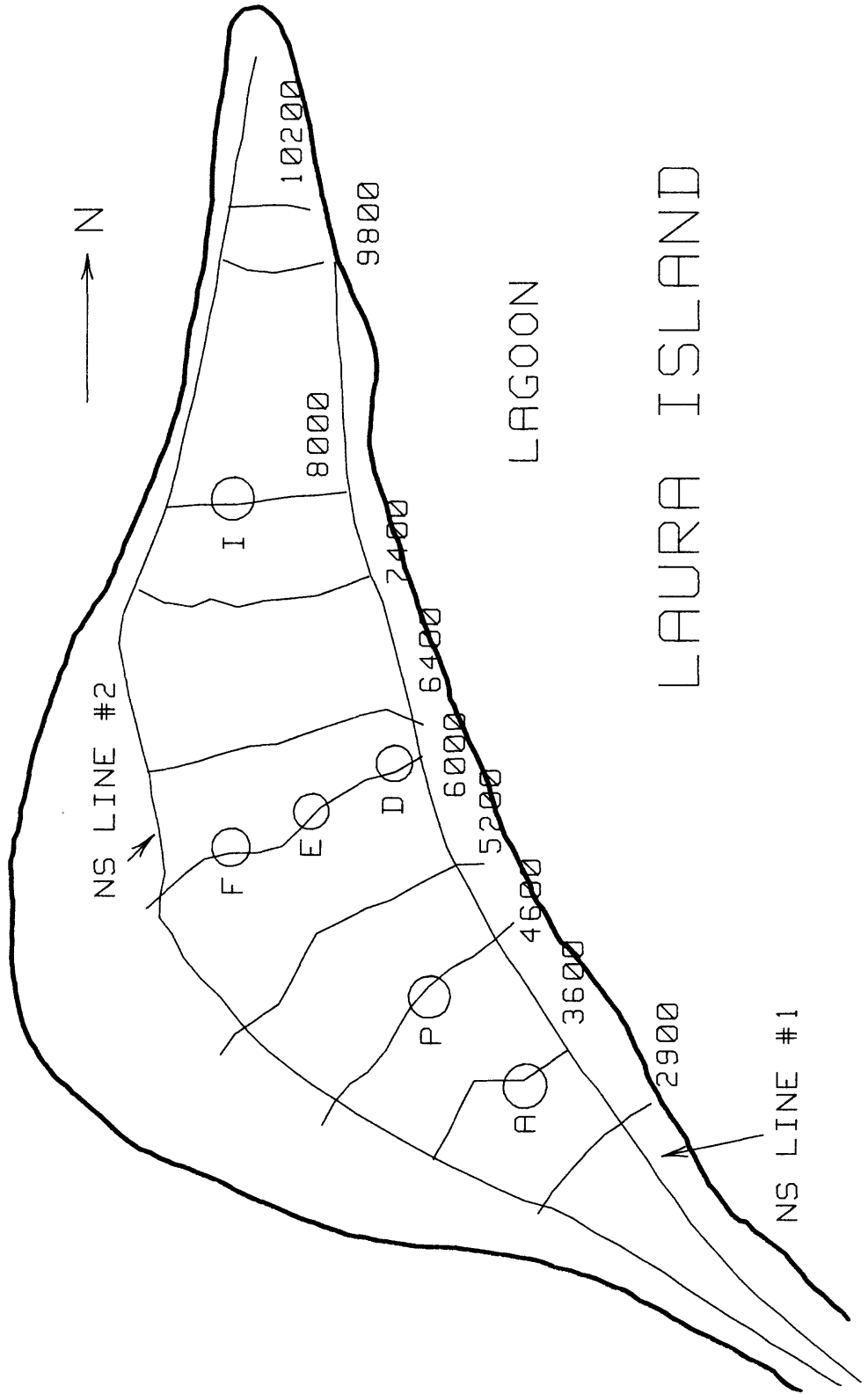


1000 10000 100 10 1 .1
RESISTIVITY (ohm-m)

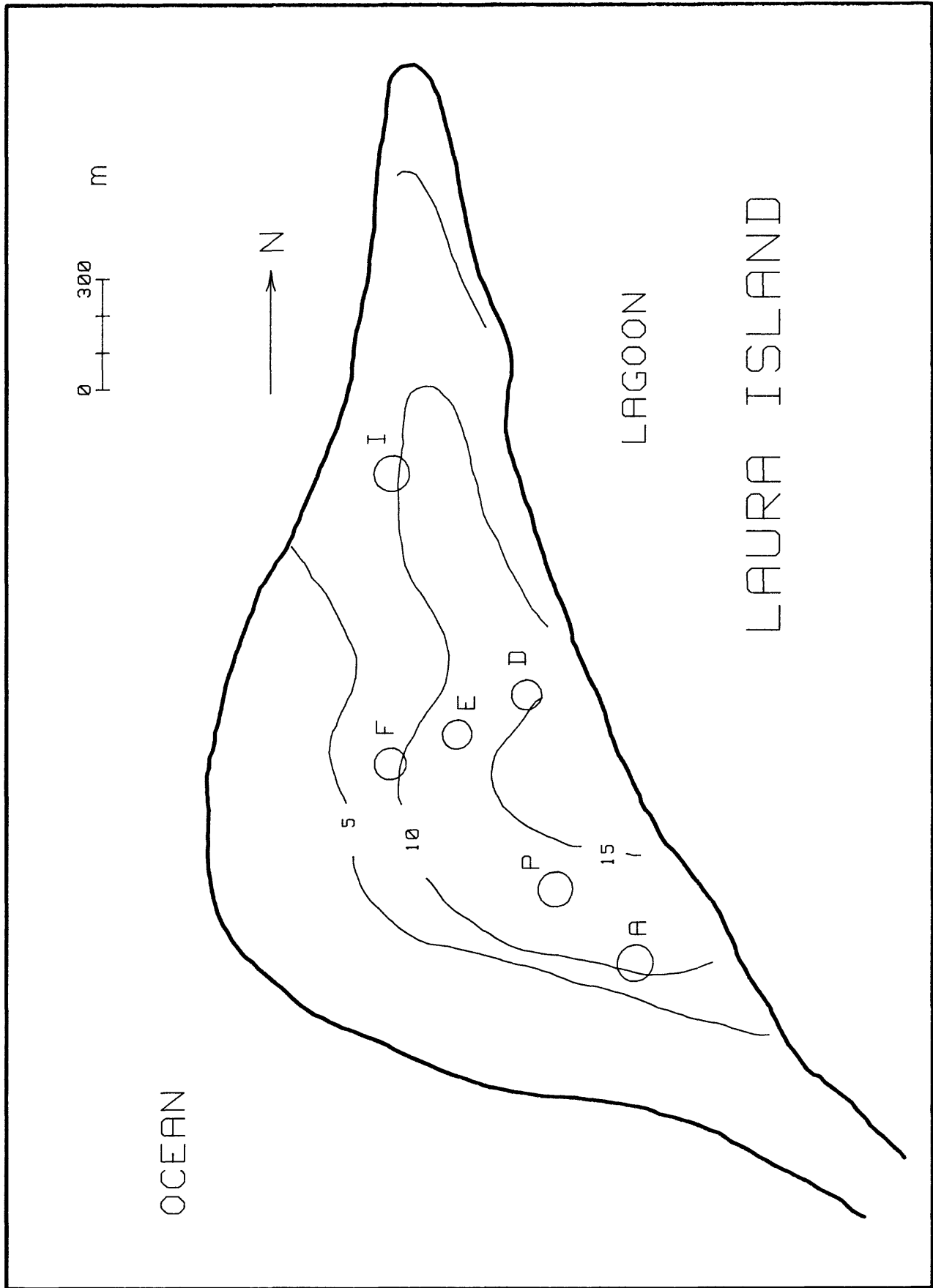
THEORETICAL SLINGRAM RESPONSES THREE LAYERS WITH TRANSITIONAL LAYER



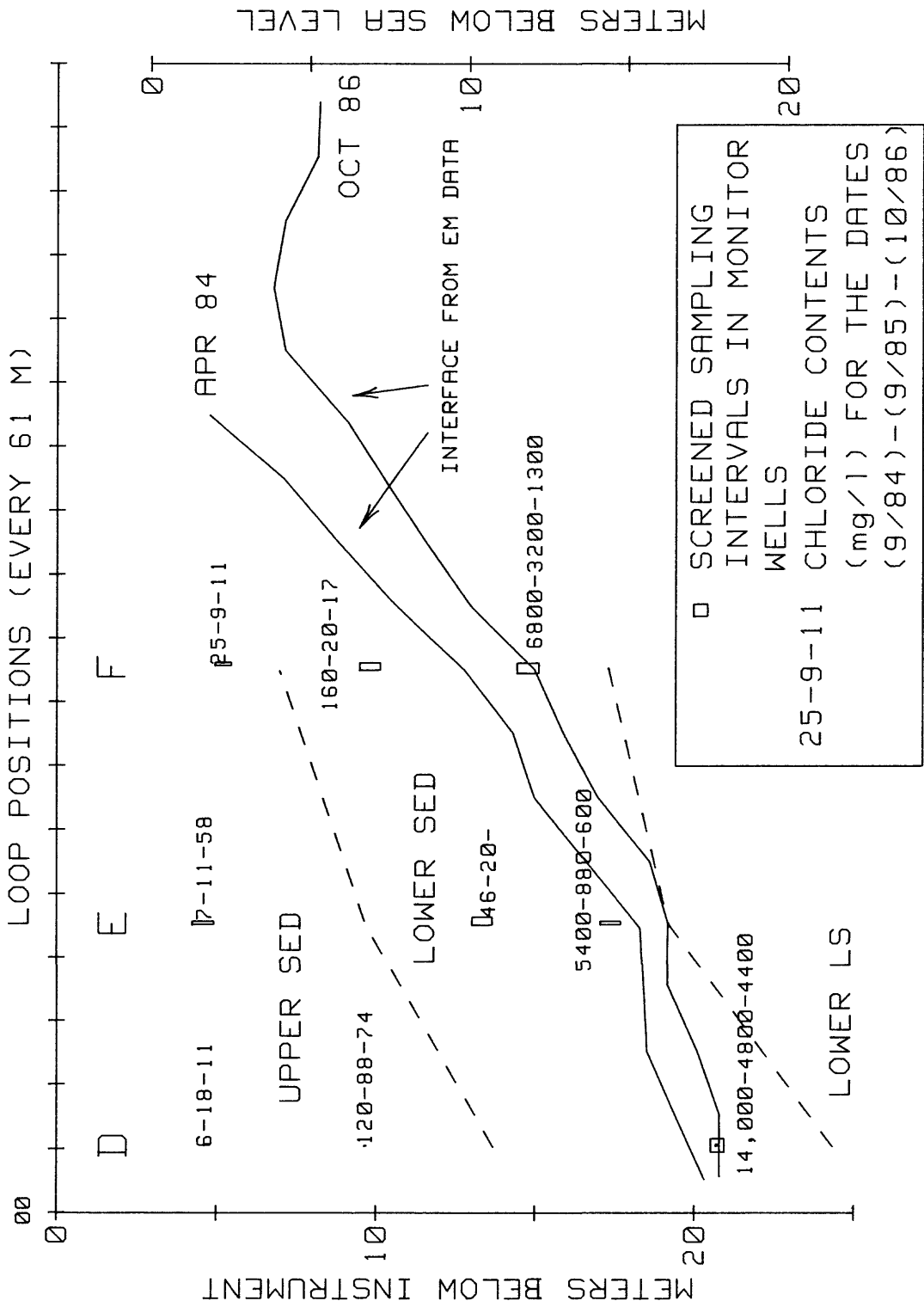
OCEAN



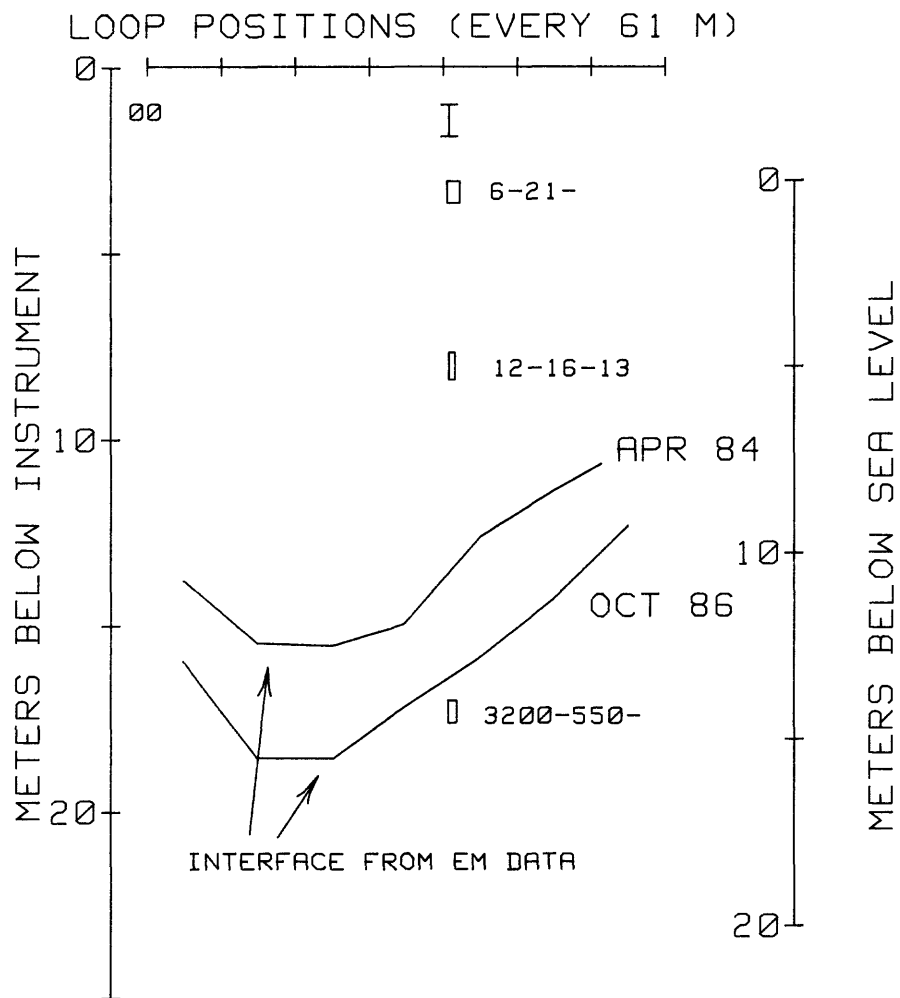
LAURA ISLAND



LINE 6000 MAJURO, MARSHALL I.



LINE 8000N MAJURO, MARSHALL I.



□ SCREENED SAMPLING INTERVALS IN MONITOR WELLS

25-9-11 CHLORIDE CONTENTS (mg/l) FOR THE DATES (9/84)-(9/85)-(10/86)

REFERENCES

- Anderson, W.A., 1979a, Program MARQDCLAG -- Marquardt inversion of DC-Schlumberger soundings by lagged convolution: U.S. Geological Survey Open-File Report 79-1432, 58 p.
- Anderson, W.A., 1979b, Program MARQLOOPS -- Marquardt inversion of loop-loop frequency soundings: U.S. Geological Survey Open-File Report 79-240, 75 p.
- Davis, S. and DeWiest, R., 1966, Hydrogeology, John Wiley & Sons, Inc., New York, 463 p.
- Glenn, W.E., Ryu, J., Ward, S.H., Peeples, W.J., and Phillips, R.J., 1973, The inversion of vertical magnetic dipole sounding data, *Geophysics*, v. 38, p. 1109-1129.
- Glenn, W.E., and Ward, S.H., 1976, Statistical evaluation of electrical sounding methods. Part I-- Experimental design, *Geophysics*, v. 41, p. 1207-1221.
- Kauahikaua, J., 1986, An evaluation of electric geophysical techniques for ground water exploration in Truk, Federated States of Micronesia, Open-File Report 87-146, 75 p.
- Keller, G.V. and Frischknecht, F., 1966, Electrical Methods in Geophysical Prospecting, Pergamon Press, Oxford, 519 p.
- Hamlin, S. and Anthony, S., 1987, Occurrence of ground water in the Laura area, Majuro Atoll, Marshall Islands, Water-Resources Investigations Report WRI 87-4047, 69 p.
- Mundry, E., 1967, The vertical magnetic field of an alternating current dipole for horizontally stratified media, *Geophysical Prospecting*, v. 15, pp. 468-479.
- Mundry, E. and Zschau, H.-J., 1983, Geoelectrical models involving layers with a linear change in resistivity and their use in the investigation of clay deposits, *Geophysical Prospecting*, v. 31, pp. 810-828.
- Parasnis, D.S., 1979, Principles of Applied Geophysics : John Wiley & Sons, New York, 275 p.

Visher, F.N. and Mink, J.F., 1964, Ground-water resources of southern Oahu, Hawaii, USGS WSP 1778, 133 p.

Wait, J.R., 1982, Geo-electromagnetism, Academic Press, New York, 268 p.